Diss. ETH No. 11277

Experimental and Numerical Investigation of Soil Vapor Extraction

A dissertation submitted to the

SWISS FEDERAL INSTITUTE OF TECHNOLOGY ZURICH

for the degree of

DOCTOR OF NATURAL SCIENCES

presented by

ULRICH FISCHER

Dipl. Geoökologe, University of Bayreuth (FRG)

born December 4, 1962

in Cologne (FRG)

accepted on the recommendation of

Prof. Dr. Rainer Schulin, examiner

Prof. Dr. Themistocles Dracos, co-examiner

Dr. Fritz Stauffer, co-examiner

1995

CONTENTS

Summary

In recent years soil vapor extraction (SVE) has been used extensively to remove volatile organic compounds (VOCs) from the vadose zone. In order to investigate processes limiting the removal of VOCs in the late stage of SVE operations, multicomponent soil venting experiments were performed at different water contents in a sand tank (80 × 66 × 5 cm) in the absence of a liquid organic phase. Four chlorinated VOCs were used as model compounds. A homogeneous packing of quartz sand was used as model soil. Gas phase concentrations were measured at several locations with different water saturation during each experiment.

The compounds did not adsorb on the sand. Volatilization was the key process for VOC removal. Gas concentrations decreased more slowly at locations with high water saturation and for compounds with small Henry's law constant. Gas concentrations observed in experiments conducted at low water content were found to be a function of dimensionless time. Tailing of gas concentrations was attributed solely to diffusion in interparticle water and suggested that local nonequilibrium conditions prevailed at large dimensionless times.

This hypothesis was examined by comparison of experimental results and numerical simulations obtained with two mathematical models which differ in the description of gas-water mass transfer: the local equilibrium approach and first-order kinetics. All parameters used in the simulations, except for the mass transfer coefficients between the aqueous phase and the gas phase, were determined independently.

The degree of nonequilibrium in the experiments was found to be a function of dimensionless time. For compounds with a large Henry's law constant the equilibrium model matched the gas concentrations measured at early times during experiments conducted at low water saturation but failed to describe the observed tailing. The kinetics model described these experimental data quite well if calibrated mass transfer coefficients were used. It was shown

that the gas-water mass transfer coefficient in the kinetics model cannot be expected to be a constant under the conditions of soil vapor extraction. The results of the numerical simulations confirm the hypothesis that mass transfer from the aqueous phase into the gas phase can be limited by diffusion within the interparticle water.

ZUSAMMENFASSUNG

Bodenluftabsaugung ist ein in den letzten Jahren häufig eingesetztes Verfahren, um leichtflüchtige Verbindungen (VOC) aus der ungesättigten Bodenzone zu entfernen. Um die bei einer Bodenluftabsaugung limitierenden Prozesse zu untersuchen, wurde das Verfahren in einem Sandtank (80 x 66 x 5 cm) nachgestellt. Die Versuche wurden ohne flüssige organische Phase durchgeführt, um das Endstadium einer Bodenluftabsaugung zu simulieren. Es wurden Mehrkomponenten-Versuche bei verschiedenen Wassergehalten durchgeführt, um den Einfluss der physiko-chemischen Parameter der Verbindungen und des Wassergehaltes auf die Entfernung der Schadstoffe zu untersuchen. Vier leichtflüchtige Chlorkohlenwasserstoffe wurden als Modellsubstanzen eingesetzt. Als Modellboden diente eine homogene Quarzsandpackung. In jedem Versuch wurden die Gaskonzentrationen der VOC an mehreren Meßstellen mit unterschiedlichem Wassergehalt gemessen.

    Die untersuchten Verbindungen adsorbierten nicht an dem Quarzsand, so daß die Verflüchtigung aus dem Wasser den für die Entfernung der Verbindungen bestimmenden Prozess darstellte. Meßstellen mit hohem Wassergehalt und Verbindungen mit niedriger Henry-Konstante zeigten geringere Konzentrationsabnahmen als Meßstellen mit niedrigem Wassergehalt und Verbindungen mit hoher Henry-Konstante. Die in Experimenten mit niedrigem Wassergehalt gemessenen Gaskonzentrationen konnten als Funktion einer dimensionslosen Zeit beschrieben werden. Das beobachtete Tailing der Gaskonzentrationen wurde alleine dem limitierenden Effekt der Diffusion in interpartikulärem Wasser zugeschrieben. Das Tailing ließ darauf schließen, daß zu großen dimensionslosen Zeiten ein lokales Ungleichgewicht zwischen der Gas- und der Wasserphase bestand.

    Diese Hypothese wurde anhand des Vergleichs gemessener Konzentrationen und numerischer Simulationen geprüft. Die numerischen Simulationen wurden mit zwei mathematischen Modellen durchgeführt, die sich in der Beschreibung des Übergangs der Verbindungen von der Wasser- in die

Gasphase unterscheiden: der Annahme lokalen Gleichgewichts, sowie Kinetik erster Ordnung. Bis auf den Massentransferkoeffizient, der im kinetischen Modell den Übergang von der Wasser- in die Gasphase beschreibt, wurden die für die Simulationen verwendeten Parameter unabhängig von den simulierten Daten bestimmt.

Das Ausmaß des Ungleichgewichts zwischen Wasser- und Gasphase entwickelte sich als Funktion der dimensionslosen Zeit. Die für Verbindungen mit hoher Henry-Konstante in Experimenten mit niedrigem Wassergehalt gemessenen Konzentrationen konnten nur zu Beginn mit dem Gleichgewichtsmodell beschrieben werden. Dieses Modell konnte die im weiteren Verlauf der Experimente gemessenen Konzentrationen nicht beschreiben. Das kinetische Modell konnte diese Daten nachvollziehen, wenn kalibrierte Massentransferkoeffizienten benutzt wurden. Es wurde gezeigt, daß der Gas-Wasser-Massentransferkoeffizient im kinetischen Modell für die Beschreibung der Bodenluftabsaugung nicht unbedingt als Konstante angenommen werden kann, sondern ebenfalls eine Funktion der dimensionslosen Zeit ist. Die Ergebnisse der numerischen Simulationen bestätigen die Hypothese, daß der Massentransfer von der Wasser- in die Gasphase durch Diffusion in interpartikulärem Wasser limitiert werden kann.

1

INTRODUCTION

In the last decades increased production of chemicals led to numerous accidential spills or leakages of chlorinated solvents and mineral oil products to the soil. These chemicals are only slightly soluble in water. The chlorinated solvents and many components of mineral oil products are volatile organic compounds (VOCs). In general VOCs have vapor pressures greater than that of water. On the other hand, tetrachloroethene - one of the five major chlorinated solvents used extensively in commerce [*Wolf et al.*, 1991] - has a vapor pressure below that of water but this compound is also characterized as volatile organic compound. Hence, the term "volatile organic compound" does not represent a strict physico-chemical definition.

In this study chlorinated VOCs were chosen as model compounds. This group of chemicals is composed of chlorinated hydrocarbons with one or two carbon atoms (methanes, ethanes, ethenes) and at least one chlorine atom. The chlorinated VOCs show excellent solvency for greases, oils, resins, and waxes. Their viscosity is about half of that of water, they have no flash point, and their density is greater than that of water. The chlorinated VOCs are widely used as solvents in a variety of industries for a range of purposes, especially for metal degreasing, dry cleaning, and animal waste processing. In comparison to aqueous solvents the chlorinated VOCs show much higher solvency for organic contaminants, and in comparison to gasoline solvents their advantage lies in the fact that fire and explosion hazards do not exist. The disadvantage of the chlorinated solvents is their high toxicity (cf. *Rippen* [1990]) which requires special measures in industrial safety management. *Fricke* [1981] and *Wolf et al.* [1991] discuss the advantages and disadvantages of alternative solvents.

Due to their high vapor pressures the chlorinated VOCs escape nearly entirely into the atmosphere [*Ballschmiter et al.*, 1987]. In the troposphere they are rapidly decomposed in a photochemical reaction with OH-radicals.

This reaction is the most important decomposition pathway for chlorinated VOCs in the environment.

In the soil spills of volatile organic compounds can induce density driven gas flow because of the high vapor pressures and molecular weights of the compounds. Due to their high liquid densities the chlorinated solvents are able to penetrate into the groundwater body if the displacement pressure is sufficiently high. The behavior of chlorinated solvent phases in the subsurface was studied experimentally by *Schwille* [1988], *Kueper et al.* [1989], and *Poulsen and Kueper* [1992].

Even small spills of chlorinated VOCs to the soil can pose a serious threat to the groundwater. Therefore, remedial measures have to be taken to clean up these spills. Soil vapor extraction (SVE), also known as soil venting, is a simple and relatively cheap in-situ technique to remove VOCs from the unsaturated zone. In recent years the number of SVE applications has increased markedly. *Travis and Macinnis* [1992] reported that SVE comprised 18 % of selected remedies at Superfund sites in the USA and that this number continued to grow. SVE is particularly suited in cases where low biodegradability or unfavourable site conditions prevent bioremediation and where, due to inaccessibility, costs, or other reasons, excavation and ex situ treatment are not practicable. The basic set-up of a soil venting operation consists of a vapor extraction well connected to a vacuum pump and a vapor treatment unit (Figure 1.1a).

The problem of soil venting operations is to direct the air flow as much as possible through the contaminated zone and to prevent short-circuiting through by-passes. Possibilities to exert control of the air flow pattern include the positioning of injection and extraction wells, the regulation of pressure, screening of wells, and sealing of the soil surface, in particular around the extraction wells to avoid short-circuiting (Figure 1.1b). The design and operation of soil venting systems is discussed in detail in *Johnson et al.* [1990] and *Wilson and Clarke* [1994].

As with all in situ techniques, a principle drawback of soil venting is the limited knowledge about the site specific subsurface characteristics (geology and hydrogeology) and the extension of the contaminated zone. Relevant knowledge about flow paths and travel times of the extracted air in the heterogeneous underground can be gained using gas tracer techniques [*Olschewski et al.*, 1995]. These results can be used to optimize the configuration and operation of the venting system.
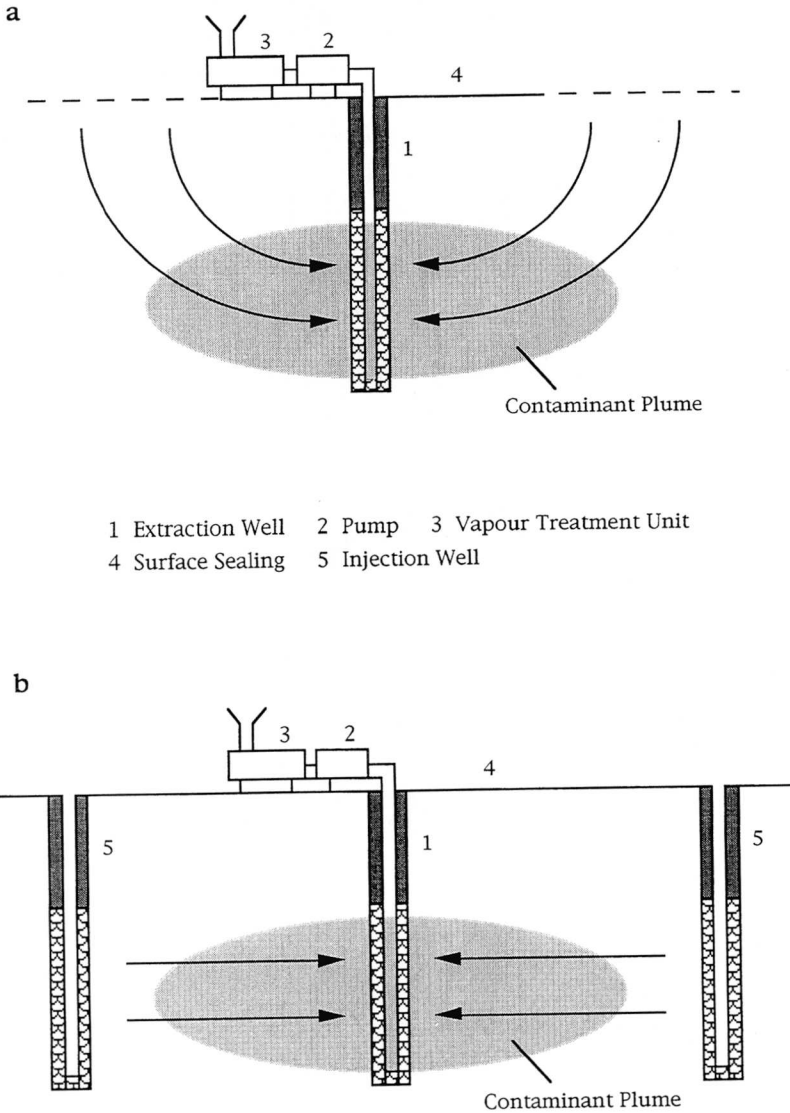
a

1 Extraction Well   2 Pump   3 Vapour Treatment Unit
4 Surface Sealing   5 Injection Well

b

Figure 1.1   *Basic set-ups of soil venting operations: a) Without air injection wells. b) With air injection wells.*

In general the efficiency of SVE operations decreases with time due to limitations in mass transfer of contaminants into the mobile gas phase. These limitations have been investigated in various experimental and numerical studies. Mass transfer from nonaqueous phase liquids (NAPLs) into the gas phase was found to be fast [e.g. *Lingineni and Dhir*, 1992; *Baehr et al.*, 1989]. In contrast, VOC removal from the dissolved and the solid phase was found to be strongly rate-limited [*McClellan and Gillham*, 1990; *Grathwohl and Reinhard*, 1993; *Wehrle and Brauns*, 1994].

The mathematical representation of mass transfer between the different phases is one of the crucial points in the formulation of a transport model. Some authors applied the local equilibrium assumption (LEA) to describe mass transfer from a NAPL or the aqueous phase into the gas phase [e.g., *Adenekan et al.*, 1994]. Alternatively non-equilibrium representations of mass transfer between gas and water were proposed which explicitly account for diffusion in the aqueous phase [*Grathwohl and Reinhard*, 1993], or assume first-order kinetics [*Gierke et al.*, 1992; *Armstrong et al.*, 1994].

Baehr et al. [1989] compared experimental SVE data with numerical simulations and concluded that the LEA is valid to describe mass transfer from the NAPL into the gas phase if the air stream passes through the contaminated region. Models based on the LEA were not adequate, however, to match the experimental data reported by *McClellan and Gillham* [1990], *Grathwohl and Reinhard* [1993], and *Wehrle and Brauns* [1994], which were obtained in the absence of a NAPL. Good descriptions were obtained in these cases with models accounting for rate-limited mass transfer [*Armstrong et al.*, 1994; *Grathwohl and Reinhard*, 1993; *Croisé et al.*, 1994].

In the present study soil vapor extraction was investigated using a tank which was filled with a quartz sand. The objective was to mimic a homogeneous porous medium without secondary porosity, where mass transfer occurs only between the aqueous phase and the gas phase. In order to investigate the influence of water saturation and of the compounds' physico-chemical properties on the removal of VOCs by soil vapor extraction, multicomponent experiments were performed, and nonuniform water contents were established in the tank. The objectives of the present study were to examine if under such experimental conditions tailing of gas concentrations can be observed indicating rate-limited mass transfer between the soil water and the gas phase, and to investigate if the experimental observations can be properly described by means of the LEA or the first-order kinetics approach. For the

latter purpose, the numerical model presented by *Armstrong et al.* [1994] was applied. In this code the LEA approach and first-order kinetics can be chosen as alternative options to describe mass transfer between gas, water, and the solid phase. On the basis of the numerical simulations the degree of nonequilibrium in the experiments was assessed by means of two parameters: the Damköhler I number [*Damköhler*, 1936], and the prefix denominator of *Bahr and Rubin* [1987] which is derived by the method of separation of the kinetically influenced term (SKIT).

2

EXPERIMENTAL PROCEDURES

In this study soil venting experiments were conducted in a sand tank. Batch and column experiments were carried out to determine physico-chemical parameters of the investigated volatile organic compounds and to characterize the quartz sand used. The chemicals used were trichloroethylene, perchloroethylene (tetrachloroethylene), 1,1,1-trichloroethane, and 1,1,2-trichloroethane. The first three compounds were chosen because they belong to the five major chlorinated solvents used extensively in commerce [*Wolf et al.*, 1991]. The last compound was selected because according to *Mackay and Shiu* [1981] this compound has a much smaller Henry's law constant than the other three solvents.

2.1 Column experiments for combined determination of water-retention characteristics and gas permeability function

A quartz sand with grain sizes in the range from 0.08 mm to 1.2 mm was used as model soil. The apparatus shown in Figure 2.1 was used to simultaneously determine the water-retention characteristics and the gas permeability function of this sand. The design of this column was adapted from *Wehrle and Brauns* [1992]. The column consisted of a porous ceramic cylinder of 15 cm length and 3 cm inner diameter (Soil Moisture Equipment, Goleta, CA, USA) enclosed in an aluminium mantle. The connection between the ceramic cylinder and the aluminium mantle at the inlet and the outlet was sealed air and water tight. The space between the wall of the ceramic cylinder and the aluminium mantle was filled with water and connected to a niveau bottle. Different matric potentials were obtained by varying the niveau. A homogeneous packing of the sand was attained by adapting the packing procedure of *Stauffer and Dracos*
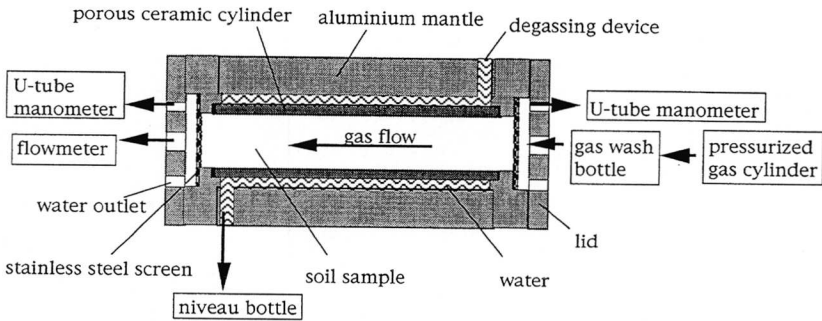
Figure 2.1 *Apparatus used to simultaneously determine the water-retention characteristics and relative gas permeability function.*

[1986]. The packing device used here allowed for free fall of the sand grains for about 50 cm followed by the passage of a series of two screens before reaching the surface of the sand body. This procedure ensured homogeneous packings and high reproducibility. The porosity of the obtained sand packing was 0.36. The sand packing was held in place by metal screens. Initially the column was held in a vertical position and saturated from the bottom. For each matric potential applied, water content and gas permeability were determined after a 24 h equilibration period. The column outlets were closed and disconnected from all tubings. Afterwards the column was weighed, and connected to a pressurized gas cylinder on one side and a soap film flow meter on the other. The rate of gas flow was measured at five pressure differences in the range from 50 Pa to 500 Pa. Pressure differences were read from a U-tube water manometer connected to the inflow and the outflow chamber of the column. Laboratory-grade air was used as fluid. In order to avoid water losses from the column, the air was moistened close to saturation using a gas-wash bottle. Water-retention curve and gas permeability were determined for drying and wetting. All experiments in this study were carried out at 22 ± 1 °C and using Nanopure water.

Measurements of the column weight were transformed into water contents by substracting the weight of the dry sand-filled column, and dividing the difference by the volume of the sand packing. The corresponding values of

matric potential and water content were used to determine the parameters of the water-retention function according to *van Genuchten* [1980] by means of the computer program RETC [*Yates et al.*, 1992]. A linear regression of the applied pressure gradients and the measured air-flow rates was calculated for each matric potential adjusted. In order to determine relative permeabilities, the slopes of the regression curves were divided by the slope obtained at residual water saturation. The threshold limit of gas flow expressed as relative gas permeability was about 4×10^{-5}. The intrinsic permeability of the sand was determined as 6×10^{-7} cm^2 by means of a separate Darcy experiment performed with cores of 5 cm inner diameter and 5 cm height.

2.2   Batch experiments for determination of Henry's law constants and solid-water distribution coefficients

Henry's law constants and water-solid distribution coefficients were determined in multicomponent batch experiments (Figure 2.2) by means of the EPICS-(Equilibrium Partitioning In Closed Systems) procedure developed by *Lincoff and Gossett* [1984], *Gossett* [1987], and *Garbarini and Lion* [1985]. In this procedure Henry's law constant of a compound is determined from the ratio of equilibrium headspace concentrations measured in two sealed bottles filled with different volumes of water [*Gossett*, 1987]. Similarly, the solid-water distribution coefficient is determined from the ratio of headspace concentrations measured in bottles with and without sorbent [*Garbarini and Lion*, 1985]. The latter procedure requires knowledge of the Henry's law constant. The EPICS-procedure has the advantage that only the ratios of added masses and measured gas phase concentrations have to be considered. Consequently, the concentration of the stock solution containing the compounds under investigation has not to be known exactly, and gas phase concentrations have not to be quantified using a calibration curve but instead measurement raw data like gaschromatographic areas can be used given a linear relationship between detector signal and concentration. Multicomponent experiments were used since *Gossett* [1987] and *Munz and Roberts* [1987] did not find a significant difference between results of one- and multicomponent experiments for the determination of Henry's law constants.
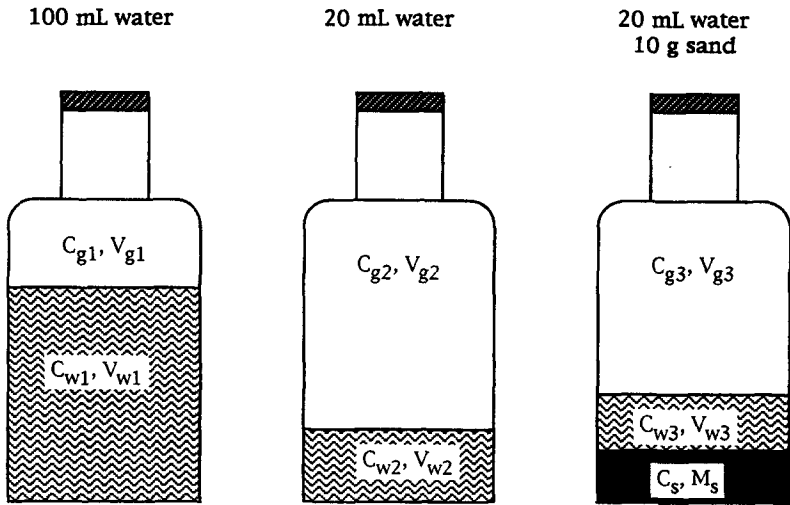
100 mL water   20 mL water   20 mL water
                                               10 g sand

C_{g1}, V_{g1} C_{g2}, V_{g2} C_{g3}, V_{g3}

C_{w1}, V_{w1} C_{w2}, V_{w2} C_{w3}, V_{w3}

                                               C_s, M_s

Figure 2.2 *Schematic representation of the different batch types used in the EPICS-procedure for the determination of the Henry's law constants and the solid-water distribution coefficients of the investigated VOCs.*

Experiments were conducted in 125 mL glass bottles (ICHEM, Newcastle, DW, USA). Three bottles were filled with about 100 mL water, three with 20 mL water, and three with 20 mL water and 10 g sand. Volumes and masses were determined gravimetrically. The screw-cap bottles were closed using teflon-lined silica septa. A stock solution was prepared by mixing 20 mL of water with excess amounts of 1,1,1-trichloroethane (1,1,1-TCA), 1,1,2-trichloroethane (1,1,2-TCA), trichloroethylene (TCE), and perchloroethylene (PCE). 4 mL of VOC saturated water were slightly diluted with 0.5 mL pure water and mixed thoroughly. The reagent-grade compounds used were purchased from Fluka (Buchs, Switzerland). By means of a syringe, 100 µL aliquots of VOC stock solution were injected through the septa of the bottles. Water concentrations in the bottles were about 1 mg L^{-1}. *Munz and Roberts* [1987] reported that Henry's law constants of halogenated VOCs were unaffected by water concentration in the range between detection limit and solubility. The bottles were vigorously shaken by hand every 30 min.

Preliminary experiments showed that three hours were sufficient to reach equilibrium between the different phases. After this time three gas samples of 100 µL each were withdrawn from each bottle using a gas-tight syringe equipped with a push-button valve (Precision Sampling, Baton Rouge, LA, USA). The concentrations of the VOCs in the samples were determined by gaschromatography (cf. Section 2.4).

For each compound nine values of the Henry's law constant and the water-solid distribution coefficient were calculated from the mass balance equations for the different batch types (cf. Figure 2.2):

$$M_1 = C_{g1} V_{g1} + C_{w1} V_{w1} \qquad (2.1)$$

$$M_2 = C_{g2} V_{g2} + C_{w2} V_{w2} \qquad (2.2)$$

$$M_3 = C_{g3} V_{g3} + C_{w3} V_{w3} + C_s M_s \qquad (2.3)$$

where the M_i are the total masses of one compound in the different batch types [M], C_{gi}, C_{wi}, and C_s represent the gas, water, and sorbed concentrations of one compound [M M^{-1}], respectively, V_{gi} and V_{wi} are the gas and water volumes [L], respectively, and M_s is the mass of sorbent in the third batch type [M]. Solving Henry's law for the water concentration gives:

$$C_{wi} = \frac{C_{gi}}{H_c} \qquad (2.4)$$

where H_c is the Henry's law constant of the compound under consideration [–]. Introducing (2.4) into (2.1) and (2.2), and combining the latter two equations yields an equation for the calculation of the Henry's law constant:

$$H_c = \frac{V_{w2}\dfrac{M_1}{M_2} - V_{w1}\dfrac{C_{g1}}{C_{g2}}}{V_{g1}\dfrac{C_{g1}}{C_{g2}} - V_{g2}\dfrac{M_1}{M_2}} \qquad (2.5)$$

The sorbed concentration C_s in (2.3) can be expressed by means of the linear sorption isotherm:

$$C_s = K_d\, C_w \tag{2.6}$$

where K_d is the solid-water distribution coefficient [L M^{-1}]. Introducing (2.6) into (2.3), and combining (2.2) and (2.3) yields the following equation for the calculation of the solid-water distribution coefficient:

$$K_d = \left[\frac{M_3}{M_2} (V_{g2}\, H_c\ +\ V_{w2}) \frac{C_{g2}}{C_{g3}} - V_{g3}\, H_c - V_{w3} \right] \frac{1}{M_s} \tag{2.7}$$

2.3   Soil vapor extraction experiments

Soil vapor extraction experiments were carried out in a tank of dimensions 80 × 66 × 5 cm. The experimental set-up is shown in Figure 2.3. In order to minimize losses of VOCs, stainless steel, glass, and teflon were used as materials for building the tank. The tank was packed with the quartz sand by means of a special device employing the same procedure as used for packing the column. Stainless steel screens which were permeable over the entire cross section separated the sand packing laterally from the injection and extraction well (cf. Figure 2.3). Glass walls enabled visual inspection of sand packing homogeneity. Twenty sampling ports with teflon-lined silica septa were installed in a rectangular grid pattern on one side of the tank. A gas-tight syringe equipped with a push-button valve was used for gas sampling. The sideport needle of the syringe was inserted through the septum of a sampling port and advanced for about 2 cm into the sand packing, and an aliquot of 100 µL gas was withdrawn. Before pulling out the syringe the push-button valve was closed to avoid dilution or losses of the sample. The concentrations of the VOC in the samples were determined by gaschromatography (cf. Section 2.4).

Gas flow was induced by means of a membrane pump (Vacuubrand, Wertheim, FRG), and measured with a flowmeter (Krohne, Duisburg, FRG). Supplied air was first dried using silica gel, then purified by activated carbon cartridges, and finally humidified to avoid water losses from the tank. The air was humidified by passing through a nebulizer cell in which two nozzles produced a very fine mist. The nebulizer cell was connected to an expansion vessel to prevent the import of water droplets into the tank. The air entering the
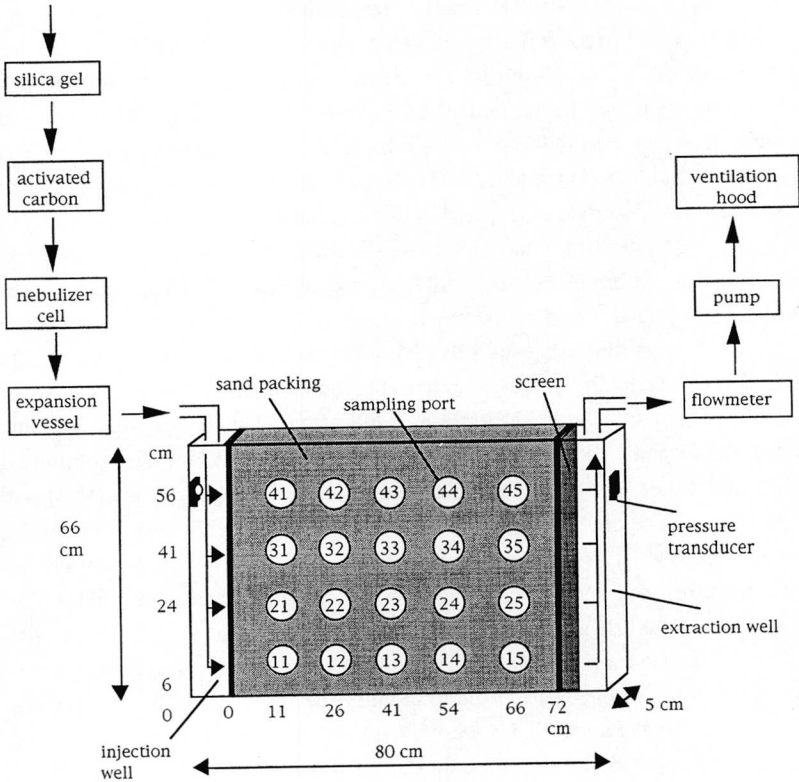
silica gel

activated carbon

nebulizer cell

expansion vessel

ventilation hood

pump

flowmeter

sand packing

sampling port

screen

cm

66 cm

56

41

24

6

0

41 42 43 44 45

31 32 33 34 35

21 22 23 24 25

11 12 13 14 15

0   11 26 41 54 66 72 cm

5 cm

pressure transducer

extraction well

injection well

80 cm

Figure 2.3   *Experimental set-up of soil vapor extraction experiments and positions of sampling ports.*

tank had a relative humidity of 98 %. Pressure transducers (Keller, Winterthur, Switzerland) were used to monitor vacuum pressures in the two wells.

Four soil venting experiments (V1 - V4) were performed in the tank. According to the profiles of water saturation and the gas flow rates established, the experiments are labeled as "dry" (V1), "moist/slow" (V2), "wet" (V3), and "moist/fast" (V4). The characteristics of these experiments are summarized in Table 2.1. The maximum degree of water saturation established in the wet

experiment (V1) was 0.30. The gas flow rate in this experiment (cf. Table 1) was of the same order of magnitude as in the moist/slow experiment V2 and the wet experiment (V3). In the moist experiments (V2, V4) the maximum water saturation was 0.54. In the moist/fast experiment (V4) the gas flow rate was initially high but then reduced after 0.5 h. In the wet experiment (V3) a water table was established at a level of 3.1 cm above the bottom of the tank. The maximum water saturation achieved in this experiment was 0.85.

Water saturations and initial VOC concentrations in the tank were established in different ways depending on the degree of water saturation to be attained. In the dry and moist experiments (V1, V2, and V4) the moisture distribution was established by infiltration of water at the top of the tank. In order to achieve hydrodynamic equilibrium, each experiment was started at the earliest three months after infiltration of the water. During this time the tank was kept closed. Water saturations were calculated from the volume of infiltrated water using the computer code MUNETOS [*Zurmühl*, 1994] and using the parameters describing the water-retention curve determined for the wetting process. The vacuum pressures in the gas phase were negligible and were not taken into account calculating matric potentials and water saturations. In order to establish a homogeneous inital distribution of the VOCs, a small volume of a liquid mixture containing all 4 compounds was released into one of the wells. Gas samples were taken to monitor the spreading of the compounds. After about 2 weeks the VOCs were evenly distributed all over the tank, and the venting experiment was started. Initial gas concentrations of the VOCs were about 1 mg L^{-1} in all venting experiments.

For the wet experiment (V3), the compounds were dissolved in water. The tank was saturated from the bottom with the VOC solution while the top lid was removed. Afterwards the water table was lowered to a level of 3.1 cm above the bottom of the tank, and the tank was closed. After an equilibration period of several days the venting experiment was started. Water saturations were calculated using the parameters describing the drying branch of the water-retention curve.

Table 2.1   Summary of soil vapor extraction experiments V1 - V4.

	V1	V2	V3	V4
	dry	moist/slow	wet	moist/fast
Porosity of sand packing [-]	0.36	0.36	0.36	0.36
Matric potential at the bottom of the tank [kPa]	-2.9¶	-1.8¶	0.31	-1.8¶
Water saturation minimum [-]	0.07	0.08	0.14	0.08
maximum [-]	0.30	0.54	0.85	0.54
Applied pressure difference [Pa]	11	14	19	240/10§
Gas flow rate [L min^{-1}]	0.60	0.82	1.0	6.6/1.0§
Extracted gas volume [m^3]	0.90	1.1	4.3	0.41
Duration of venting [h]	25	22	72	4

¶ Calculated.
§ Reduction of gas flow rate after 0.5 h.

2.4 Gaschromatographic analysis of VOCs in gas samples

The determination of VOC concentrations in the gas samples was carried out on a Hewlett Packard 5890 II gaschromatograph using split injection (split ratio 1:16; 120 °C) and electron capture detection (ECD; 300 °C). A 15 m DB-1 fused-silica capillary column (J & W Scientific, Folsom, CA, USA) with an inner diameter of 0.32 mm and 5 μm film thickness was used. Oven temperature was held constant at 104 °C. High-purity helium was used as carrier gas at a flow rate of 1.3 mL min^{-1}. In order to determine calibration curves, aliquots of the liquid VOCs were diluted in hexane, and these standards were evaporated in 125 mL glass bottles. The analysis had to be very reliable, because no replicates could be measured in the tank experiments. Precision of the analytical procedure was determined by measuring six replicates of gas standards at various concentrations in the range from 10 ng L^{-1} to 1 mg L^{-1}. Coefficients of variation in general were below 2.5 %. The highest value obtained was 4.8 %.

3

EXPERIMENTAL RESULTS

The parameters characterizing the porous medium (intrinsic permeability, water-retention characteristics, gas permeability function) and its interactions with the compounds (solid-water distribution coefficients) were obtained from independent experiments. Also the Henry's law constants of the investigated VOCs were determined independently. Own measurements of the Henry's law constants were made since for the compounds here under study wide ranges of values for this key parameter were found in the literature [e.g., *Mackay and Shiu*, 1981]. The results obtained in these experiments are presented in the following two sections. In the last section of this chapter the results of the soil vapor extraction experiments are presented.

3.1 Water-retention characteristics and gas permeability function

The water-retention curves of the quartz sand packing observed for drying and wetting are shown in Figure 3.1a. The relationship between matric potential and water saturation was clearly hysteretic. During wetting water saturation for a given matric potential was lower than during drying. The parameter values of the water-retention functions fitted to the model of *van Genuchten* [1980] for the drying and wetting branches of the retention data are given in Table 3.1. The parameter m was fixed as $1-1/n$.

Relative gas permeabilities obtained for drying and wetting are shown in Figure 3.1b. The relationship between water saturation and relative gas permeability again was clearly hysteretic. At a given water saturation relative gas permeability observed for the wetting process was higher than that determined for the drying process. This result agrees with the finding of *Stonestrom and Rubin* [1989b] for Oakley sand, and contradicts the statement

of *Luckner et al.* [1989] claiming that observations of numereous studies imply
that wetting and nonwetting permeabilities are single-valued and nonhysteretic.
Stonestrom and Rubin [1989b] introduced the terms "emergence point" for the
water saturation at which gas flow becomes detectable during drying, and
"extinction point" for the water saturation at which measurable gas flow
disappears during wetting. The emergence and extinction points for the data
presented in Figure 3.1b are 0.58 and 0.66, respectively. The lowest non-zero
permeability determined was about 100 times higher than the threshold limit.
This result indicates the abruptness of gas permeability emergence and
extinction. The emergence and extinction points observed by *Stonestrom and
Rubin* [1989b] for Oakley sand were somewhat higher but qualitatively the
findings of the two studies agree quite well. It can be concluded that
knowledge of the gas permeability function is of major importance for modeling
SVE operations when regions with high water saturation are considered.

The phase distribution and relative permeability model employed in the
simulations of the present study is shown schematically in Figure 3.2. It is
based on the concept presented by *Luckner et al.* [1989]. Their concept was
based on the work of *van Genuchten* [1980] and *Mualem* [1976], and accounts
for the nonwetting phase residual saturation. *Luckner et al.* [1989] defined
both wetting and nonwetting phase residual saturation as the maximum degree
of saturation with zero permeability for the respective phase. According to
Luckner et al. [1989] the residual gas saturation $S_{g,r}$ corresponds to the gas-
permeability emergence or extinction point $S_{w,e}$ (cf. Figure 3.2). The
experimentally determined emergence and extinction points of gas flow differed
from the maximum water saturation achieved. Thus, the ranges of effective gas

Table 3.1   *Parameters of the phase distribution and relative
permeability model represented by Equations (3.1) - (3.5).*

	α [cm⁻¹]	n [-]	m [-]	$S_{w,r}$ [-]	$S_{w,e}$ [-]	$S_{g,r}$ [-]	$S_{g,r}^{*}$ [-]
Drying	0.032	4.0	0.75	0.04	0.58	0.42	0.15
Wetting	0.056	3.1	0.68	0.04	0.66	0.34	0.15
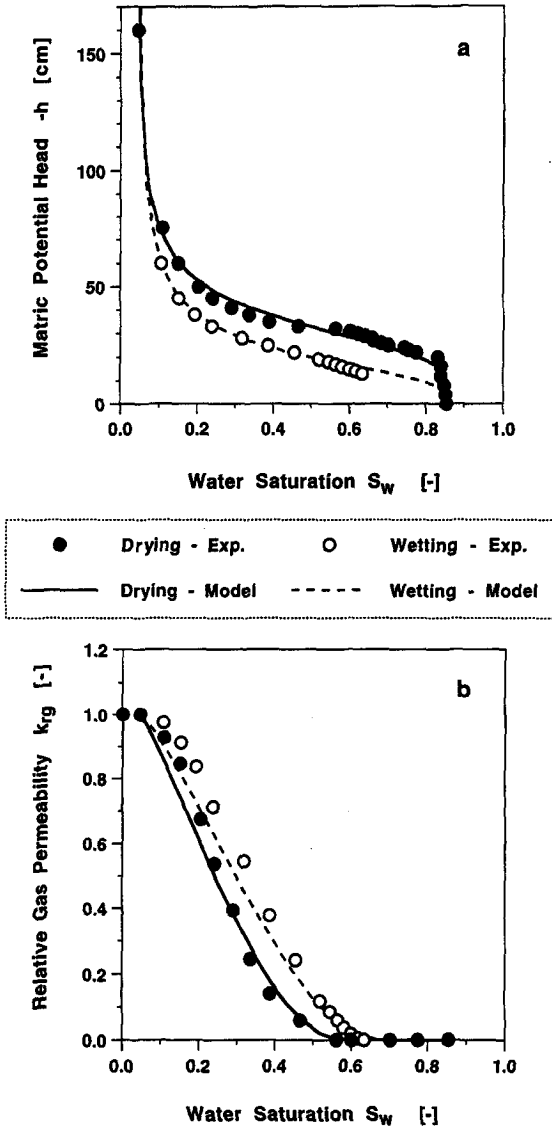
Figure 3.1 *Characteristics of quartz sand packing determined for drying and wetting. Experimental results and curves fitted to the model represented by Equations (3.1) - (3.5) are shown: a) Water-retention curves. b) Relative gas permeability.*
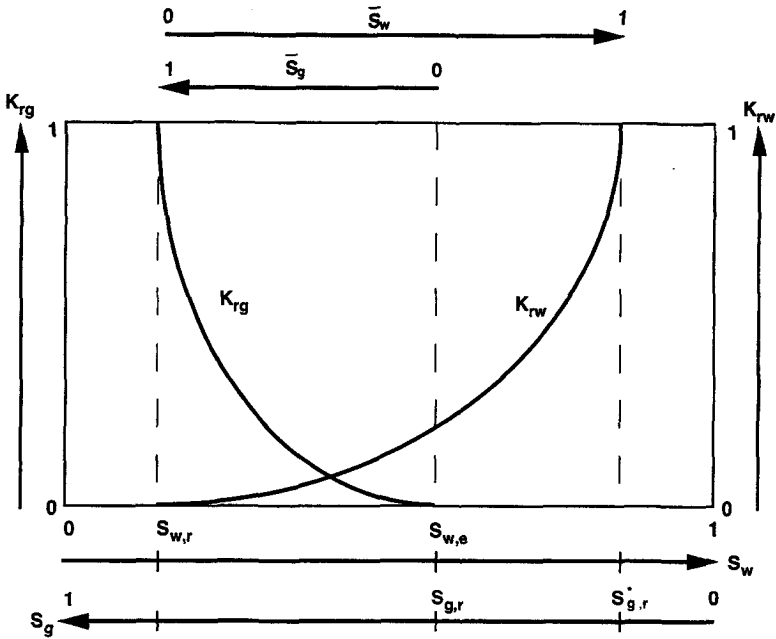
Figure 3.2 *Schematic representation of the relative permeability functions of gas (K_{rg}) and water (K_{rw}) as defined by Equations (3.1) - (3.5). The residual gas saturation $S_{g,r}$ is not assumed to be identical for wetting and drying.*

saturation $\overline{S}_g$ and effective water saturation $\overline{S}_w$ were not identical (cf. Figure 3.2). To account for this difference an apparent residual gas saturation $S_{g,r}^*$ was introduced into the model which defines the gas saturation at maximum water saturation (cf. Figure 3.2).

In the mathematical framework used in the present study the effective water saturation $\overline{S}_w$ [-] is modeled according to *van Genuchten* [1980] as:

$$\overline{S}_w = (1 + (\alpha h)^n)^{-m} \qquad (3.1)$$

where h is the matric potential head [L], and α [L^{-1}], n [-], and m [-] are empirical parameters. The water saturation S_w [-] and the gas saturation S_g [-] are

calculated considering the apparent residual gas saturation $S_{g,r}^*$ [-] at maximum water saturation:

$$S_w = \overline{S}_w (1 - S_{w,r} - S_{g,r}^*) + S_{w,r} \qquad (3.2)$$

$$S_g = 1 - S_w \qquad (3.3)$$

where $S_{w,r}$ is the residual saturation of water [-]. The volumetric phase contents are obtained by the relationships $\theta_w = S_w \, \varepsilon$, and $\theta_g = S_g \, \varepsilon$, where ε is the soil porosity [-]. The effective gas saturation $\overline{S}_g$ [-] is calculated as:

$$\overline{S}_g = \frac{S_g - S_{g,r}}{1 - S_{w,r} - S_{g,r}} \quad for \ \ S_{g,r} < S_g < 1 - S_{w,r} \qquad (3.4a)$$

$$\overline{S}_g = 0 \quad for \ \ S_g < S_{g,r} \qquad (3.4b)$$

where $S_{g,r}$ [-] is the residual gas saturation corresponding to the gas permeability emergence or extinction point. In the range $S_{g,r}^* < S_g < S_{g,r}$ the gas phase is discontinuous and, thus, a considerable volume of gas is trapped. *Stonestrom and Rubin* [1989a] assumed that the main mechanisms inducing changes in the trapped gas content are expansion and compression of gas, and occlusion and liberation of gas resulting from water blockage formation and destruction. In the present study gas expansion and compression can be neglected because of the small pressures under consideration. Further investigations are required in order to explain the process of gas entrapment.

Relative gas permeability k_{rg} [-] and relative water permeability k_{rw} [-] were calculated using $\overline{S}_g$ and $\overline{S}_w$, respectively, and applying the van Genuchten-Mualem model [*Mualem*, 1976; *van Genuchten*, 1980]:

$$k_{rg} = \overline{S}_g^{\ 1/2} (1 - (1 - \overline{S}_g)^{1/m})^{2m} \qquad (3.5a)$$

$$k_{rw} = \overline{S}_w^{\ 1/2} (1 - (1 - \overline{S}_w^{\ 1/m})^m)^2 \qquad (3.5b)$$

The values of $S_{g,r}$ determined for drying and wetting (cf. Table 3.1) were 0.42 and 0.34, respectively, and the values of $S_{w,r}$ and $S_{g,r}^*$ were 0.04 and 0.15, respectively.

3.2 Henry's law constants and solid-water distribution coefficients

The Henry's law constants and solid-water distribution coefficients of the VOCs determined in the batch experiments are given in Table 3.2 together with other physico-chemical properties of the compounds. Henry's law constant H_c in its dimensionless form is defined as:

$$H_c = \frac{C_g}{C_w} \qquad (3.6)$$

where C_g and C_w denote the gas and water concentration [M L^{-3}] of a compound, respectively. Henry's law refers to phase equilibrium and is valid for dilute concentrations. The temperature dependence of H_c can be described as [*Gossett*, 1987; *Munz and Roberts*, 1987]:

$$log\ H_c = A - B\frac{1}{\tau} \qquad (3.7)$$

where A [-] and B [K] are empirical parameters, and τ is absolute temperature [K]. Only within a small range of temperature the parameters A and B can be considered as constant. Because of the temperature dependence, single values of H_c are only valid at those temperatures at which they have been determined. The values of the dimensionless Henry's law constants for 1,1,1-TCA and PCE determined in this study (0.73 ± 0.03 and 0.69 ± 0.02, respectively) are of comparable magnitude. The value for TCE (0.45 ± 0.02) is somewhat lower, whereas the value for 1,1,2-TCA (0.09 ± 0.01) is markedly below the other values. Except for the value of 0.37 [*Mackay and Shiu*, 1981] values for 1,1,2-TCA reported in the literature are in the range between 0.03 and 0.05 [*Mackay and Shiu*, 1981; *Dilling*, 1977]. The values of H_c for the three other compounds determined in the present study agree well within those reported by *Lincoff and Gossett* [1984], *Gossett* [1987], and *Munz and Roberts* [1987].

The values of the solid-water distribution coefficients K_d determined with the quartz sand for the four VOCs were not significantly different from zero. Thus, adsorption of the four VOCs on the quartz sand was considered to be negligible under wet conditions. This result is in agreement with the findings of *Krause* [1987] and *Gierke et al.* [1992] who observed no adsorption of TCE

Table 3.2 *Physico-chemical properties of 1,1,1-trichloroethane (1,1,1-TCA), 1,1,2-trichloroethane (1,1,2-TCA), trichloroethylene (TCE), and perchloroethylene (PCE) at 22 °C and 1 atm.*

	1,1,1-TCA	1,1,2-TCA	TCE	PCE	Reference
Molecular weight [g mol^{-1}]	133.4	133.4	131.4	165.8	(1)
Henry's law constant [-]	0.73	0.09	0.45	0.69	(2)
Solid-water distribution coefficient [cm^3 g^{-1}]	0	0	0	0	(2)
Solubility (20 °C) [g L^{-1}]	1.55	4.36	1.08	0.149	(3)
Gas diffusion coefficient [cm^2 s^{-1}]	8.56×10^{-2}	8.56×10^{-2}	8.80×10^{-2}	8.04×10^{-2}	(4)
Water diffusion coefficient [cm^2 s^{-1}]	8.57×10^{-6}	8.57×10^{-6}	8.91×10^{-6}	8.02×10^{-6}	(5)

References: (1) *Weast* [1989]; (2) *this work*; (3) *Horvath* [1982]; (4) Calculated according to *Wilke and Lee* [1955]; (5) calculated according to *Hayduk and Laudie* [1974].

and toluene, respectively, on wet quartz sands. As no interaction between the VOCs and the quartz sand was found also competitive sorption could be neglected. *Gossett* [1987] and *Munz and Roberts* [1987] reported no difference between values of Henry's law constants determined in single- and multicomponent experiments. Therefore, it was assumed that in the multicomponent soil venting experiments conducted in this study interactions between the VOCs themselves were negligible, and that the experimental results are equivalent to those of one-component experiments.

3.3 Soil vapor extraction experiments

The characteristics of the four soil venting experiments V1 - V4 are summarized in Table 2.1. The vertical profiles of water saturation established in the experiments are shown in Figure 3.3. Positions of sampling ports (SP) are given in Figure 2.2.

Influence of water saturation and Henry's law constant

Figure 3.4 shows the gas phase concentrations of the four VOCs measured at sampling port SP 13 during the moist/slow experiment (V2). The water saturation at this location was 0.38. After 8 h of pumping the relative concentrations of 1,1,1-TCA, TCE, and PCE had decreased to values below 0.1, whereas the relative concentration of 1,1,2-TCA still was close to unity. The concentration of PCE was slightly higher than that of 1,1,1-TCA. TCE showed a higher concentration than PCE. At this stage the magnitudes of the relative concentrations of the four VOCs were inversely related to the respective Henry's law constants (cf. Table 3.2). After 22 h the difference between the concentrations of 1,1,2-TCA and the other three compounds was as pronounced as after 8 h. The relative concentration of 1,1,2-TCA was about 0.5. Values of about 0.01 were determined for the other compounds. 1,1,1-TCA still showed the lowest concentration. Despite the different Henry's law constants of TCE and PCE their concentrations were nearly identical and somewhat higher than the concentration of 1,1,1-TCA.
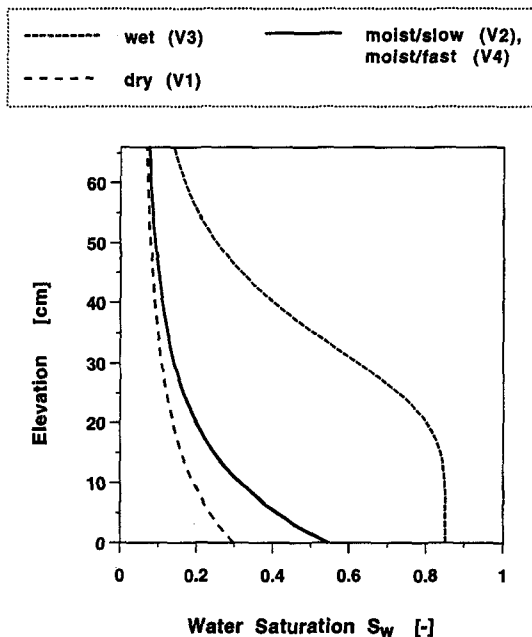
Figure 3.3 *Calculated profiles of water saturation S_w in soil venting experiments V1 - V4.*

Courses of relative concentration obtained for 1,1,1-TCA, TCE, and PCE were quite similar in all experiments, and were clearly different from those observed for 1,1,2-TCA. For simplicity, therefore, only the concentrations of TCE and 1,1,2-TCA observed in the dry experiment (V1), in the moist/slow experiment (V2), and in the wet experiment (V3) are presented in this chapter (Figures 3.5 - 3.7). The concentrations of PCE and 1,1,1-TCA are shown in Figures A.1 - A.3 in the Appendix. Each plot shows the concentrations of one compound at three or four sampling ports during one experiment. The sampling ports were located at the same horizontal distance from the air-entry well but at different elevations (cf. Figure 2.1), and thus, at points of different water saturation (cf. Figure 3.3). Each of the Figures 3.5 - 3.7 represents one
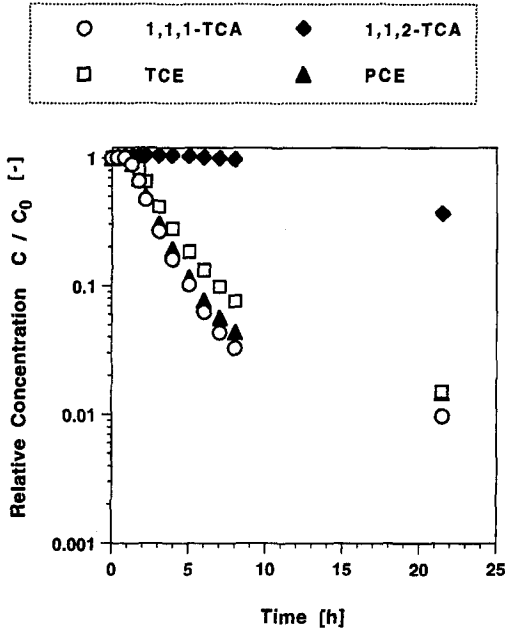
Figure 3.4   *Relative gas concentrations of the four VOCs investigated at sampling port SP 13 during the moist/slow soil vapor experiment (V2). Note coincidence of last measurements for TCE and PCE.*

experiment with the concentrations of TCE in the left plot and those of 1,1,2-TCA in the right plot. In the wet experiment (V3) the concentration of 1,1,2-TCA at sampling ports SP 42 and SP 32 quickly fell below the detection limit. Water saturation and average linear velocity at each sampling port are given in the legend. Average linear velocities v [L T^{-1}] were calculated from Darcy's law using the best-fit relationships between water saturation and relative gas permeability:

$$v = \frac{q}{\theta_g} = - k_{rg} \, k_i \, \frac{1}{\theta_g \, \mu_g} \, \frac{\Delta p}{\Delta x} \qquad (3.8)$$

where q is the Darcy velocity [L T^{-1}], θ_g is the volumetric gas content [-], k_{rg} is the relative gas permeability [-], k_i is the intrinsic permeability [L^2], μ_g is the dynamic gas viscosity [M L^{-1} T^{-1}], Δp is the difference between exit and entry gas pressure [M L^{-1} T^{-2}], and Δx is the distance between the two wells [L]. Vertical profiles of average linear velocity are shown in Figure 3.8. In the wet experiment (V3) advective gas flow occured only at elevations above 32 cm. Below this elevation water saturation exceeded the value of gas permeability emergence obtained for drying (0.58). In the dry experiment (V1) average linear velocity varied only little with elevation and was nearly constant at elevations above 20 cm.

The narrowest range and lowest values of water saturation were established in experiment V1, whereas in experiment V3 the highest values and the widest range of water saturation were achieved (cf. Figure 3.3). Courses of relative concentration obtained at different sampling ports varied more in the wet experiment (V3) than in the moist/slow experiment (V2), and variation was least in the dry experiment (V1). It has to be taken into account that the applied pressure differences were not exactly the same in the three experiments (cf. Table 2.1). Thus, linear velocities were not identical at the same water saturation in different experiments. Nevertheless, concentration courses measured at different sampling ports during one experiment, and those of different experiments with different ranges of water saturation clearly show the high influence of water saturation on the gas phase concentrations of the VOCs. Even small differences in water saturation in the range close to the residual water saturation caused quite large differences in the respective concentrations in the initial stage of the experiment (cf. experiment V1, Figure 3.5). On the other hand, the concentrations of TCE at different sampling ports with low water saturation converged for later stages of the experiments. At the end of experiments V1 (dry) and V2 (moist/slow) concentrations of TCE measured at sampling ports SP 23, SP 33, and SP 43 were nearly identical. In the wet experiment (V3) concentrations of TCE measured at SP 32 and SP 42 coincided after 70 h. The results obtained at SP 13 in the dry experiment (V1) and in the moist/slow experiment (V2), and at sampling port SP 22 in the wet experiment (V3) show that for high water saturations differences in gas concentration are conserved over large time periods.

For 1,1,2-TCA the influence of water saturation on the courses of relative gas concentration was much more pronounced than for TCE (Figures 3.5 - 3.7).
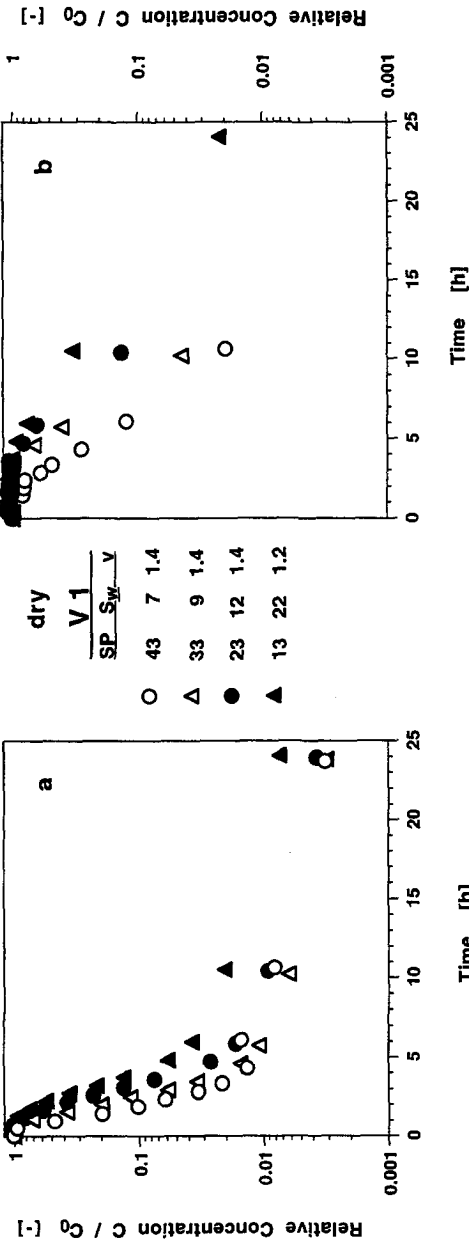
Figure 3.5 *Relative gas concentrations of trichloroethylene (a) and 1,1,2-trichloroethane (b) at several sampling ports (SP) during the dry soil vapor extraction experiment (V1). Water saturation S_w [%] and average linear velocity v [$\times 10^{-2}$ cm s^{-1}] at each sampling port are given in the legend.*
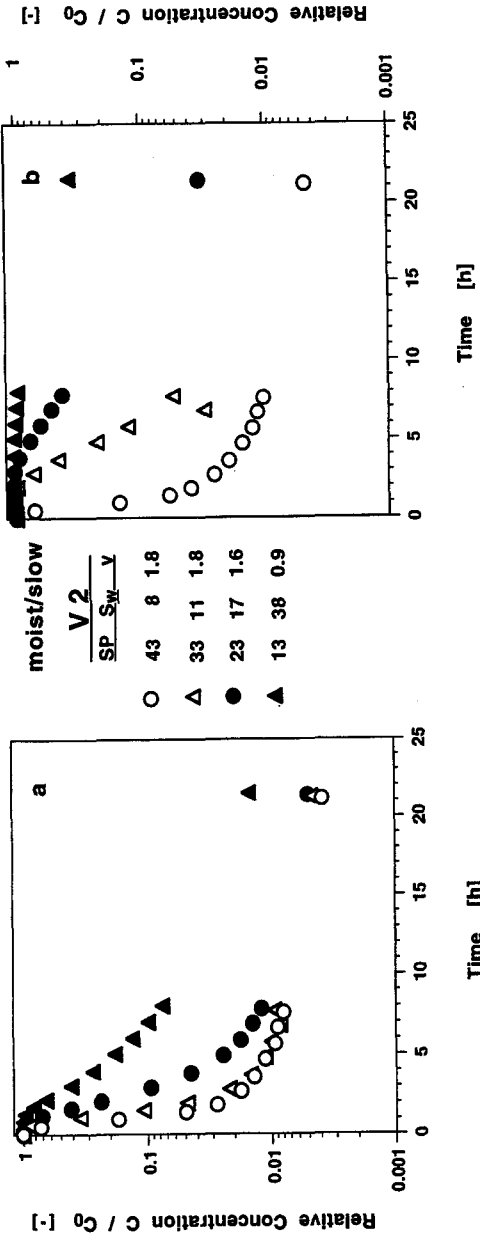
Figure 3.6 *Relative gas concentrations of trichloroethylene (a) and 1,1,2-trichloroethane (b) at several sampling ports (SP) during the moist/slow soil vapor extraction experiment (V2). Water saturation S_w [%] and average linear velocity v [$\times 10^{-2}$ cm s^{-1}] at each sampling port are given in the legend.*
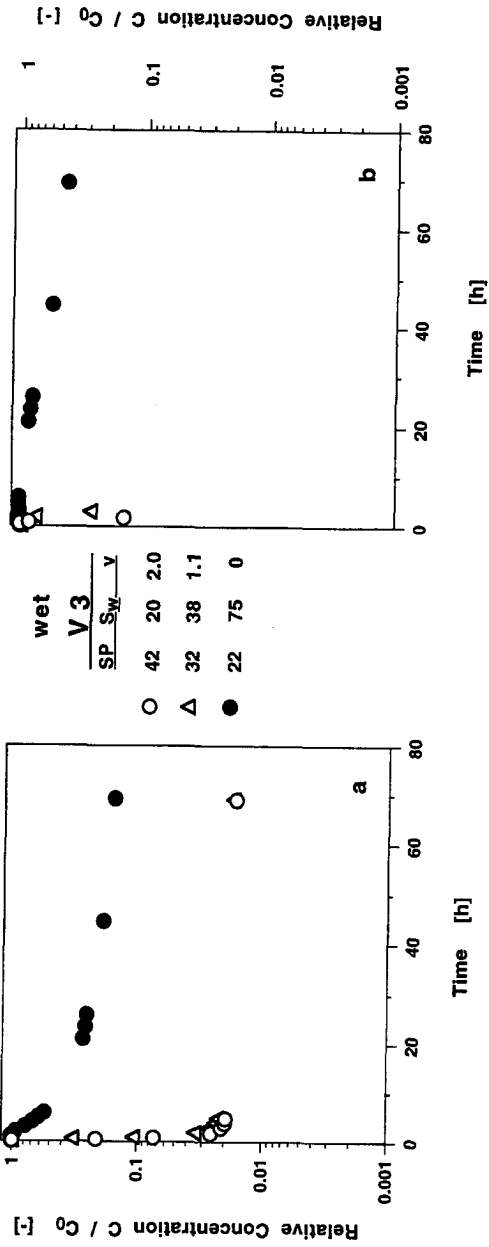
Figure 3.7 *Relative gas concentrations of trichloroethylene (a) and 1,1,2-trichloroethane (b) at several sampling ports (SP) during the wet soil vapor extraction experiment (V3). Water saturation S_w [%] and average linear velocity v [× 10^{-2} cm s^{-1}] at each sampling port are given in the legend. Note coincidence of last measurements for TCE at SP 32 and SP 42.*

A comparison of corresponding curves obtained for TCE and 1,1,2-TCA demonstrates the influence of the Henry's law constant (Figures 3.5 - 3.7). In all experiments and at all sampling ports the concentration of TCE decreased faster than that of 1,1,2-TCA. Differences between the concentrations of the two compounds generally were smaller at low water saturations. In the dry experiment (V1) and in the moist/slow experiment (V2) they agreed more at sampling port SP 43 than at SP 13, and generally agreed more in the dry experiment (V1) than in the moist/slow experiment (V2). Corresponding concentrations of both compounds measured at sampling ports with low water saturation converged in the late stage of the experiments. At SP 43 in the moist/slow experiment (V2) the relative concentrations of both compounds were nearly identical at the end of the experiment.

Due to a water saturation of 0.75 no advective gas flow occured at sampling port SP 22 in the wet experiment (V3). At this location the declines in gas concentration were controlled by diffusion. Diffusion coefficients of the four compounds are of comparable magnitude (cf. Table 3.2) but the difference in the Henry's law constant led to different retardation of the compounds. Therefore, the decrease in gas concentration of 1,1,2-TCA at SP 22 was smaller than that of TCE. Both concentration courses indicate that mass removal from domains where advective gas flow was zero proceeded only slowly.

After an equilibration period of several days following shutdown of the pump in experiments V1, V2, and V3 gas concentrations were measured in the tank. The mass retained in the tank was calculated using the Henry's law constants of the compounds and the known volumes of water and gas. The sum of VOC masses was taken as a measure of VOC removal. In the wet experiment (V3) the tank was vented for 70 h (4.3 m^3 gas extracted). After this time 72 % of the initial VOC mass were extracted from the tank. In the moist/slow experiment (V2) 92 % were removed within 22 h (1.1 m^3 gas extracted), and in the dry experiment (V1) 97 % were vented within 25 h (0.9 m^3 gas extracted). These results confirm the importance of water saturation on the removal of VOCs by soil vapor extraction. The tailing of the concentration courses shown in Figures 3.5 - 3.7 indicates that it would have taken quite long to remove the remaining masses.

In the moist/fast experiment (V4) the initial rate of gas flow was rather high. Gas concentrations quickly fell below the detection limits. After 0.5 h of venting, gas flow was reduced from 6.6 to 1.0 L min^{-1}. The reduction of gas
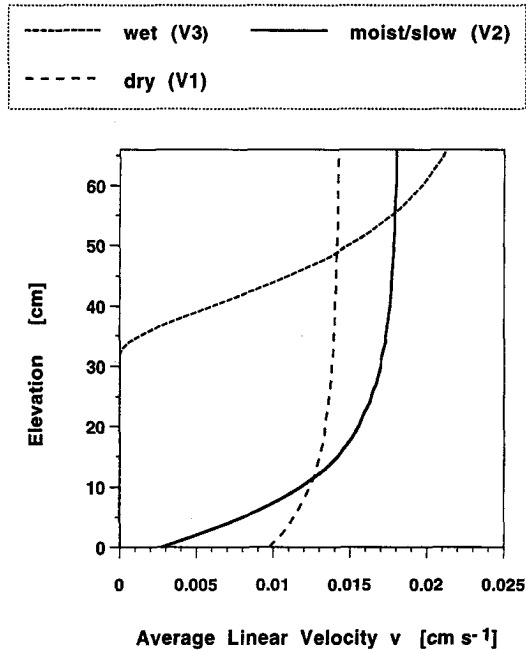
Figure 3.8   *Calculated profiles of average linear velocity v in soil vapor extraction experiments V1 (dry), V2 (moist/slow), and V3 (wet).*

flow led to temporary raises in gas concentrations of all compounds. In Figure 3.9 the concentrations of PCE measured at sampling ports SP 11 and SP 21 are shown. The period of concentration increase is followed by a slow decrease in gas concentration. The relatively fast raises in gas concentration following reduction of the flow rate suggest that mass transfer of VOCs from the water to the gas was initially slow compared to transport in the gas phase, and that the two phases were not under local equilibrium conditions.
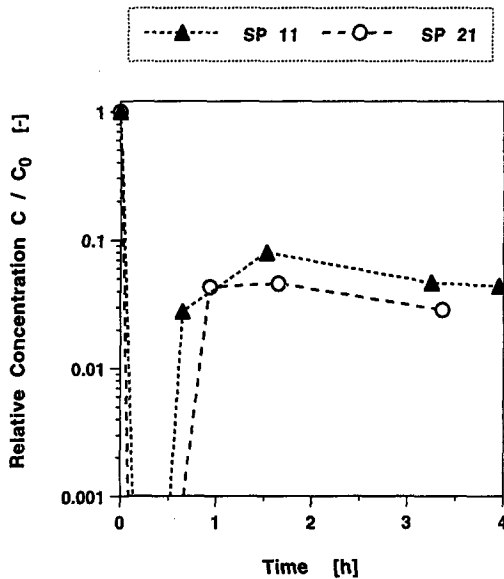
Figure 3.9 *Relative gas concentration of perchloroethylene at two sampling ports (SP) during the moist/fast soil vapor extraction experiment (V4). After 0.5 h of venting, gas flow was reduced from 6.6 to 1.0 L min^{-1}.*

Analysis of tailing behavior by time scaling

The courses of relative concentration observed in the dry experiment (V1) and in the moist/slow experiment (V2) which were conducted at low water saturations differed considerably (cf. Figures 3.5 and 3.6) but in general they had the same shape which is characterized by a steep initial decline and a long tail. This is shown in Figure 3.10a where the concentration courses (32 in total) of the four compounds observed at each four sampling ports in experiments V1 (dry) and V2 (moist/slow) are scaled to a dimensionless time T defined as:

$$T = \frac{v\,t}{L\,R} \tag{3.9}$$

where v is the average linear velocity of the gas [L T^{-1}], t is time [T], L is a reference length [L] chosen as the distance between the two wells, and R [-] is the retardation factor for gas phase transport defined as [*Armstrong et al.*, 1994]:

$$R = 1 + \frac{\theta_w}{\theta_g H_c} + \frac{\rho_b K_d}{\theta_g H_c} \qquad (3.10)$$

where θ_g and θ_w are the volumetric gas and water content [-], respectively, H_c is the Henry's law constant [-], K_d is the solid-water distribution coefficient [L^3 M^{-1}], and ρ_b is the soil bulk density [M L^3]. The last term on the right-hand side of (3.10) was zero since the solid-water distribution coefficients were zero (cf. Table 3.2). The scaled courses of relative concentration presented in Figure 3.10a agree quite well. For values of T below 2 they exhibit a linear decrease. All curves show a sharp transition at T equal to 2 and approach constant values signifying long tailing. The different slopes of the curves in the range of T below and above 2 indicate that two different processes were involved. The high coincidence of all curves suggests that gas concentrations observed for different compounds and at different locations during the two experiments were controlled by the same processes governed by the factors defining T, namely water saturation, linear velocity, and Henry's law constant. This is also shown in Figure 3.10b where only the last measurement C_E/C_0 of each curve presented in Figure 3.10a is displayed as a function of the corresponding dimensionless time T_E. These data represent the function between relative concentration and dimensionless time quite well. As a result of the small Henry's law constant of 1,1,2-TCA the last measurements for this compound had not yet reached the stage of slow mass removal (Figure 3.10b).

The compounds did not adsorb on the quartz sand. Hence, volatilization was the key process for VOC removal. *Gierke et al.* [1992] concluded that film resistance at the interface is not of importance for mass transfer between gas and water. Hence, it is assumed that diffusion within the interparticle water was the limiting process for VOC removal from the aqueous phase. The water formed films on the nonporous sand grains, and wedges between them (Figure 3.11). The extension and the exact geometry of the films and the wedges depended on the degree of water saturation. In general, the mean distance from the gas-water interface was greater for the wedges than for the films (cf.
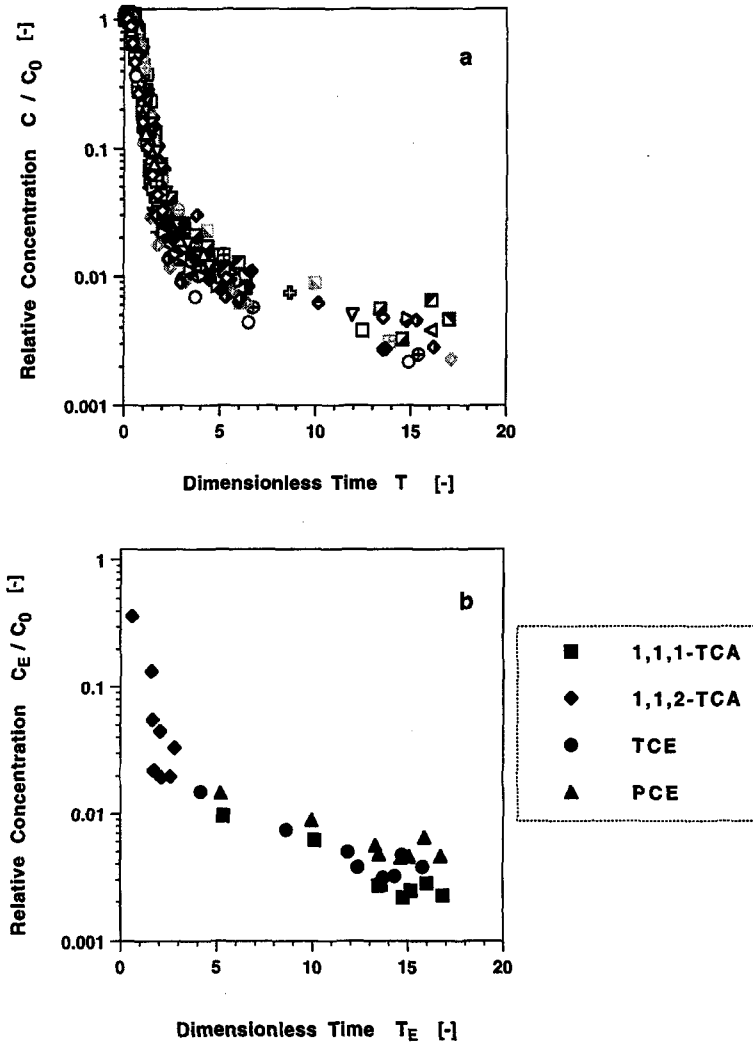
Figure 3.10   *Relative concentrations of 1,1,1-TCA, 1,1,2-TCA, TCE, and PCE recorded at four sampling ports during the dry soil vapor extraction experiment (VI) and the moist/slow experiment (V2). Relative concentrations are plotted as a function of dimensionless time as defined in Equation (3.9): a) All measurements of the 32 observations; symbols are not defined because of the large number of data sets. b) Endpoint values C_E/C_0 of the curves displayed in Figure 3.10a plotted as a function of dimensionless time T_E; measurements for the same compound are shown with the same symbol.*
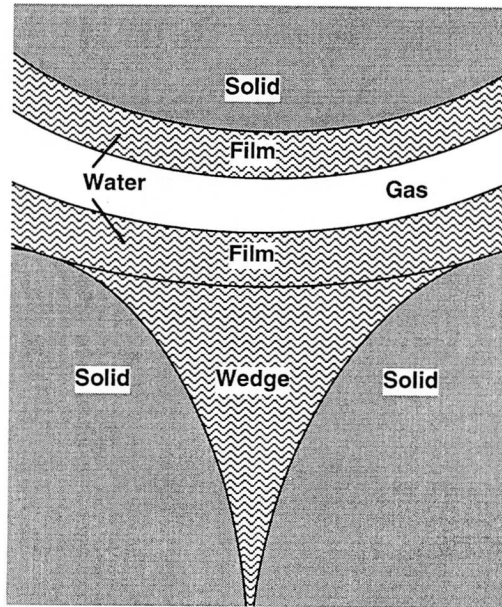
Figure 3.11 *Schematic representation of the distribution of gas and water in a granular porous medium consisting of nonporous particles without secondary porosity. The interparticle water is subdivided into films and wedges.*

Figure 3.11). Therefore, mass removal from the films probably proceeded much faster than removal from the wedges. The steep inital decrease in gas concentration may correspond to removal of VOCs from the films, whereas the tailing may correspond to removal from the wedges. The tailing indicates that transport in the gas phase proceeded much faster than mass transfer into the gas phase, and that local nonequilibrium conditions prevailed in the SVE experiments. In Chapter 5 this hypothesis is tested by comparison of experimental results and numerical simulations obtained with two different

models for gas-water mass transfer: the local equilibrium approach, and first order kinetics.

Nonequilibrium transport and long tailing behavior of VOC removal from wet sands during SVE experiments conducted in the absence of a liquid organic phase were also reported by *McClellan and Gillham* [1990], *Grathwohl and Reinhard* [1993], and *Wehrle and Brauns* [1994]. In these studies it was concluded that nonequilibrium was due to sorption processes, diffusion in intraparticle water, or a combination of both mechanisms. *Gierke et al.* [1992] concluded from comparison of experimental data and mathematical simulations that toluene vapor transport in Ottawa sand was not subject to nonequilibrium effects. In their experiments toluene was not adsorbed on the wet sand. Thus, the processes controlling VOC removal probably were the same as in the present study. Contrary to the results reported by *Gierke et al.* [1992], the results presented in this paper show that solely diffusion within the interparticle water can cause tailing of gas concentrations during soil vapor extraction.

4

NUMERICAL MODEL

In the present study the numerical model of *Armstrong et al.* [1994] was used. It was based on the model developed by *Mendoza and Frind* [1990]. In order to apply the model of *Armstrong et al.* [1994] to the experiments presented in Section 3.3, the following assumptions were made. The porous medium was considered to be incompressible. Isothermal conditions were assumed because the variations of temperature in the experiments were in the range of ±1 °C. The experiments were simulated by means of a two-dimensional model because it was assumed that no gradients appeared in direction of the third dimension (horizontal-transversal) of the narrow tank. Multicomponent experiments were modeled as superpositions of one-component simulations since it was assumed that results of multicomponent experiments were equivalent to those of one-component experiments (cf. Section 3.2). The experiments were carried out in the absence of a liquid organic phase so that

$$S_o = 0 \qquad (4.1)$$

where S_o is the saturation of the liquid organic phase [-]. The aqueous phase was considered stagnant, and water saturation was assumed to be time-invariant. This assumption appeared to be justified because vacuum pressures applied and the resulting changes in matric potential were small, evaporation and condensation could be neglected, and sources and sinks were not present in any of the phases. Therefore, the continuity equation for the aqueous phase is

$$\varepsilon \frac{\partial \rho_w S_w}{\partial t} = 0 \qquad (4.2)$$

where ε is the soil porosity [-], ρ_w is the density of water [M L^{-3}], S_w is the water saturation [-], and t is time [T].

4.1 Gas flow equations

Using the double index summation convention [*Bear*, 1972], the continuity equation for the gas phase can be written as:

$$\varepsilon \frac{\partial \rho_g \, S_g}{\partial t} = - \frac{\partial \rho_g \, q_i}{\partial x_i} \quad i,j = 1, 2 \tag{4.3}$$

where ρ_g is the gas density [M L^{-3}], the x_i denote the spatial coordinates [L], and q_i is the Darcy velocity in i-direction [L T^{-1}]:

$$q_i = - \frac{k_{rg} \, k \, \rho_0 \, g}{\mu_g} \left(\frac{\partial h^*}{\partial x_j} + \rho_{rg} \, \frac{\partial z}{\partial x_j} \right) \tag{4.4}$$

where k_{rg} is the relative gas permeability [-], k is the intrinsic permeability [L^2], ρ_0 is a reference gas density [M L^{-3}], e.g., that of pure air, g is gravitational acceleration [L T^2], μ_g is dynamic gas viscosity [M L^{-1} T^{-1}], $h*$ is called the equivalent fresh air head [L], z is elevation [L], and ρ_{rg} is defined as relative deviation of gas density from the reference gas density:

$$\rho_{rg} = \frac{\rho_g}{\rho_0} - 1 \tag{4.5}$$

Darcy's law can be used to describe gas flow because the effects of slip flow (Klinkenberg effect) are negligible in silts, sands, and gravels [*Massmann,* 1989] and for pressure gradients as small as they were established in the experiments conducted in this study [*McWhorter*, 1990]. The equivalent fresh air head $h*$ is defined as [*Mendoza and Frind*, 1990]:

$$h^* = \frac{p}{\rho_0 \, g} + z \tag{4.6}$$

where p denotes the gas pressure [M L^{-1} T^{-2}]. Combining (4.3) and (4.4), using (4.6), and assuming negligible gas density variations in space and time-invariant

gas saturations leads to the flow equation for the gas phase solved by the numerical model of *Armstrong et al.* [1994]:

$$\frac{\partial}{\partial x_i}\left[\frac{k_{rg}\,k\,\rho_0\,g}{\mu_g}\left(\frac{\partial h^*}{\partial x_j}+\rho_{rg}\,\frac{\partial z}{\partial x_j}\right)\right]=S_s\,\frac{\partial h^*}{\partial t} \qquad (4.7)$$

where the specific storativity S_s [L^{-1}] is defined as [*Mendoza and Frind*, 1990]:

$$S_s=\theta_g\,\rho_0\,g\,\gamma \qquad (4.8)$$

where γ is gas compressibility [L T^2 M^{-1}].

The relationships between matric potential and water saturation, and between water saturation and gas permeability as represented by Equations (3.1) - (3.5) were incorporated into the numerical model of *Armstrong et al.* [1994]. The initial condition was specified as:

$$h^*(x_i,0)=h_0(x_i) \qquad (4.9)$$

where $h_0(x_i)$ are the initial values of equivalent head of air [L]. No-flux boundary conditions were used along the top and the bottom of the simulated domain, and Dirichlet-type boundary conditions (type 1) were used for the in- and outflow boundary:

$$h^*(x_i,t)=h_1^*(x_i) \quad on\;\Gamma_1\;\;(inflow) \qquad (4.10a)$$

$$h^*(x_i,t)=h_2^*(x_i) \quad on\;\Gamma_2\;\;(outflow) \qquad (4.10b)$$

where $h_1^*(x_i)$ and $h_2^*(x_i)$ are the values of equivalent head prescribed on the inflow and the outflow boundary, respectively.

4.2 Transport equations

In the experiments presented in Section 3.3 the investigated chlorinated VOCs were neither produced nor consumed to a significant extent. Due to continuous venting with fresh air, aerobic conditions prevailed during the experiments. Aerobic biodegradation of the investigated chlorinated VOCs in

sandy soils has not been reported in the literature. Two studies reported abiotic degradation rates for 1,1,1-trichloroethane. *Klecka et al.* [1990] found a rate of about 0.0005 d^{-1} using aquifer samples (solids and water), and *Vogel and McCarty* [1987] observed rates of 0.0001 - 0.0005 d^{-1} in groundwater samples stored in the laboratory. These results signify that abiotic transformations as well as biodegradation could be neglected in modeling the soil venting experiments. As a consequence, the decay terms in the mass conservation equations were set to zero. The mass conservation equation for one compound in the sorbed phase for this case is:

$$\rho_b \frac{\partial C_s}{\partial t} = N_s \qquad (4.11)$$

where ρ_b is the soil bulk density [M L^{-3}], C_s is the concentration in the solid phase [M M^{-1}], N_s is the mass-transfer rate per porous medium volume to (+) or from (-) the sorbed phase [M L^{-3} T^{-1}].

As in the numerical model of *Armstrong et al.* [1994] the water is considered to be stagnant and diffusion in this phase is neglected, the mass conservation equation for one compound in the aqueous phase is:

$$\theta_w \frac{\partial C_w}{\partial t} = N_w \qquad (4.12)$$

where θ_w is the volumetric water content [-], C_w is the water concentration [M L^{-3}], and N_w is the mass-transfer rate per porous medium volume to (+) or from (-) the aqueous phase [M L^{-3} T^{-1}].

Mass conservation of one species in the gas phase can be written as:

$$\theta_g \frac{\partial C_g}{\partial t} = -\frac{\partial J_i}{\partial x_i} + N_g \qquad (4.13)$$

where θ_g is volumetric gas content [-], C_g is gas concentration [M L^{-3}], and J_i is the mass flux density of the compound under consideration in the gas phase in the i-direction per porous medium cross-section [M L^{-2} T^{-1}], N_g is the mass-transfer rate per porous medium volume to (+) or from (-) the gas phase [M L^{-3} T^{-1}]. The mass flux density J_i is assumed to be convection-dispersion in the model of *Armstrong et al.* [1994], that is:

$$J_i = C_g \, q_i - \theta_g \, D_{ij} \frac{\partial C_g}{\partial x_j} \tag{4.14}$$

where D_{ij} is the dispersion tensor $[L^2 \, T^{-1}]$. The dispersion tensor represents mechanical dispersion and molecular diffusion, and is defined according to *Bear* [1972] using the tortuosity correction of *Millington* [1959]:

$$D_{ij} = \left[\lambda_T |q| \, \delta_{ij} + (\lambda_L - \lambda_T) \frac{q_i \, q_j}{|q|} \right] \theta_g^{-1} + \frac{\theta_g^{7/3}}{\varepsilon^2} D_0 \tag{4.15}$$

where λ_L and λ_T are the longitudinal and transverse dispersivity of the porous medium $[L]$, respectively, δ_{ij} is the Kronecker delta, $|q|$ is the absolute value of the Darcy velocity $[L^2 \, T^{-1}]$, and D_0 is the molecular diffusion coefficient in free gas $[L^2 \, T^{-1}]$.

The use of Fick's first law for describing molecular diffusion in (4.14) is not adequate in systems where contributions of Knudson diffusion and nonequimolar diffusion are significant. According to *Thorstenson and Pollock* [1989] the contributions of Knudson diffusion are negligible except for very fine grained materials, and nonequimolar diffusion can be neglected for dilute concentrations.

Combination of (4.13) and (4.14) yields the convection-dispersion equation (CDE) for gas phase transport:

$$\theta_g \frac{\partial C_g}{\partial t} = \frac{\partial}{\partial x_i} \left(\theta_g \, D_{ij} \frac{\partial C_g}{\partial x_j} \right) - q_i \frac{\partial C_g}{\partial x_g} + N_s \tag{4.16}$$

As no sources and sinks were present in the system, the sum of the net mass-transfer rates for the different phases was equal to zero:

$$N_g + N_w + N_s = 0 \tag{4.17}$$

Introducing (4.11), (4.12), and (4.16) into (4.17) gives the phase-summed transport equation:

$$\theta_g \frac{\partial C_g}{\partial t} + \theta_w \frac{\partial C_w}{\partial t} + \rho_b \frac{\partial C_s}{\partial t} = \frac{\partial}{\partial x_i} \left(\theta_g \, D_{ij} \frac{\partial C_g}{\partial x_j} \right) - q_i \frac{\partial C_g}{\partial x_g} \equiv L(C_g) \tag{4.18}$$

where $L(C_g)$ is the differential operator denoting the convective and dispersive terms.

Mass transfer between the different phases can be modeled in various ways, e.g., by means of the local equilibrium assumption (LEA), first-order kinetics, or explicit diffusion formulations. The numerical model of *Armstrong et al.* [1994] allows independent choices between LEA and first-order kinetics to describe both the mass transfer between the gas and the aqueous phase, as well as between the water and the solid phase. In the simulations presented hereafter mass transfer between the aqueous phase and the solid phase was always chosen to follow the LEA. However, this choice was not of importance for the simulation results because the solid-water distribution coefficients were zero (cf. Section 3.2). Mass transfer between the gas phase and the aqueous phase was described by either the LEA or first-order kinetics as indicated in each case. The two choices of using the transport model are referred to here as the equilibrium model and the kinetics model.

The assumption of local equilibrium means that mass transfer between the different phases is fast in comparison to transport so that the concentrations in the different phases are locally in thermodynamic equilibrium, and thus related by equilibrium partitioning coefficients. In the equilibrium model the concentrations in the gas phase and the aqueous phase are linked according to Henry's law:

$$C_g = H_c \, C_w \qquad (4.19)$$

where H_c is the compounds Henry's law constant [-]. The relationship between water and sorbed concentration is given by the linear sorption isotherm

$$C_s = K_d \, C_w \qquad (4.20)$$

where K_d is the water-solid distribution coefficient [$L^3 \, M^{-1}$]. With (4.19) and (4.20) the transport Equation (4.18) yields

$$R \, \theta_g \frac{\partial C_g}{\partial t} = \frac{\partial}{\partial x_i} \left(\theta_g \, D_{ij} \frac{\partial C_g}{\partial x_j} \right) - q_i \frac{\partial C_g}{\partial x_i} \qquad (4.21)$$

where R is the retardation factor for gas-phase transport [*Armstrong et al.,* 1994]:

$$R = 1 + \frac{\theta_w}{\theta_g \, H_c} + \frac{\rho_b \, K_d}{\theta_g \, H_c} \qquad (4.22)$$

Armstrong et al. [1994] assumed that the application of the first-order kinetics approach to the description of mass transfer between gas and water approximates the following conceptual model. Diffusive mass transfer between the aqueous phase and the gas phase takes place through a boundary layer which is part of the water. The gradient between the average concentration in the water and the equilibrium concentration at the gas-water interphase is the driving force for the diffusive mass transfer between the two phases. The transport equation for the gas phase in the kinetics model is:

$$\theta_g \, \frac{\partial C_g}{\partial t} + \theta_g \, \lambda_{gw} \left(C_g - H_c \, C_w \right) = L(C_g) \qquad (4.23)$$

where λ_{gw} is the gas-water mass transfer coefficient [T^{-1}]. Assuming equilibrium sorption the storage equation for the water-solids phase is [*Armstrong et al.,* 1994]:

$$\theta_w \, R_s \, \frac{\partial C_w}{\partial t} = \theta_g \, \lambda_{gw} \left(C_g - H_c \, C_w \right) \qquad (4.24)$$

where R_s is the water-solid retardation factor [-]:

$$R_s = 1 + \frac{\rho_b \, K_d}{\theta_w} \qquad (4.25)$$

The following initial condition was applied here with respect to transport:

$$C_g(x_i, 0) = C_0 \qquad (4.26)$$

where C_0 is the uniform gas concentration [M L^{-3}] measured in the tank before starting the pump. A Cauchy-type boundary condition (type 3) was stipulated at the inflow boundary, and a Neuman-type boundary condition (type 2) was defined at the outflow boundary:

$$\left(-\theta_g D_{ij} \frac{\partial C_g}{\partial x_j} + \theta_g v_i C_g \right) n_i = 0 \quad on \ \Gamma_1 \ (inflow) \tag{4.27}$$

$$n_i D_{ij} \frac{\partial C_g}{\partial x_j} = 0 \quad on \ \Gamma_2 \ (outflow) \tag{4.28}$$

where n_i represents the unit vector normal to the boundary.

4.3 Numerical representation

The model of *Armstrong et al.* [1994] uses the Galerkin method with triangular elements and linear basis functions to solve the flow and transport equations. In order to incorporate the mass transfer relationships directly into the gas phase transport equation, the technique of *Leismann et al.* [1988] is used. With this technique, only the gas phase transport equations (in matrix form) need to be solved simultaneously, while the dissolved phase and sorbed phase equations can be solved explicitly. Further details are given by *Armstrong et al.* [1994]. These authors also tested the code against an analytical solution. They concluded that the numerical model solves the governing equations correctly. No further numerical model testing ("verification") was carried out in the present study.

5

NUMERICAL SIMULATIONS

In this chapter the experimental results presented in Section 3.3 are compared to numerical simulations. The compounds' Henry's law constants and solid-water distribution coefficients, as well as the intrinsic permeability, the water-retention characteristics, and the relative gas permeability function of the quartz sand were determined by means of independent experiments (cf. Chapter 2). Only mass transfer coefficients λ_{gw} were calibrated separately for each set of data. Thus, mass transfer coefficients were used in a descriptive and not a predictive sense.

The vacuum pressures which were measured in the two wells of the tank were specified as boundary conditions. Zero mass flux was stipulated at the inlet boundary, and a zero concentration gradient at the outlet boundary. VOC concentrations which were measured before starting the soil venting experiments were specified as initial conditions. The parameter values which were used for the numerical simulations are given in Tables 5.1 and 5.2. A rectangular grid with 18 nodes in the vertical direction, and 14 nodes in the horizontal direction was used to represent the experimental system. The positions of the nodes were chosen to coincide with the sampling ports of the sand tank (cf. Figure 2.3).

5.1 Comparison of equilibrium model and kinetics model

In Figure 5.1 the equilibrium model and the kinetics model are compared for the dry experiment (V1; cf. Table 5.1) with TCE (cf. Table 5.2). The gas-water mass transfer coefficient of the kinetics model was varied over three orders of magnitude (10^{-4} s^{-1} - 10^{-7} s^{-1}). Results are presented as graphs of normalized gas concentration, water concentration, and total mass in the domain against

Table 5.1   *Parameter values used for modeling soil vapor extraction experiments V1 - V4.*

	V1 dry	V2 moist/slow	V3 wet	V4 moist/fast	Ref.
Length of domain [cm]	72	72	72	72	(1)
Height of domain [cm]	66	66	66	66	(1)
Temperature [$^{\circ}$C]	22 ±1	22 ±1	22 ±1	22 ±1	(1)
Porosity [-]	0.36	0.36	0.36	0.36	(1)
Bulk density [g cm^{-1}]	1.68	1.68	1.68	1.68	(1)
Residual water content [-]	0.016	0.016	0.016	0.016	(1)
Residual gas content [-]	0.12	0.12	0.15	0.12	(1)
α - van Genuchten model [cm^{-1}]	0.056	0.056	0.032	0.056	(1)
n - van Genuchten model [-]	3.1	3.1	4.0	3.1	(1)
m - van Genuchten model [-]	0.68	0.68	0.75	0.68	(1)
Matric head at lower bound. [cm]	-29	-18	3.1	-18	(1)
Intrinsic permeability [cm^2]	6×10^{-7}	6×10^{-7}	6×10^{-7}	6×10^{-7}	(1)
Longitudinal dispersivity [cm]	7	7	7	7	(2)
Transversal dispersivity [cm]	0.7	0.7	0.7	0.7	(3)
Air viscosity [Pa s]	1.82×10^{-5}	1.82×10^{-5}	1.82×10^{-5}	1.82×10^{-5}	(4)
Pressure difference § [Pa]	11	14	19	240/10	(1)
Duration of venting [h]	25	22	72	4	(1)

§ Between in- and outflow boundary.

References: (1) *this work*; (2) estimated as 0.1 × length of domain; (3) estimated as 0.1 × longitudinal dispersivity; (4) according to *Bird et al.* [1960].

Table 5.2 *Physico-chemical parameters of 1,1,1-trichloroethane (1,1,1-TCA), 1,1,2-trichloroethane (1,1,2-TCA), trichloroethylene (TCE), and perchloroethylene (PCE) used for modeling soil vapor extraction experiments.*

	1,1,1-TCA	1,1,2-TCA	TCE	PCE	Reference
Molecular weight [g mol^{-1}]	133.4	133.4	131.4	165.8	(1)
Henry constant [-]	0.73	0.09 / 0.04§	0.45	0.69	(2)
Solid-water distribution coefficient [cm^3 g^{-1}]	0	0	0	0	(2)
Gas diffusion coefficient [cm^2 s^{-1}]	8.56×10^{-2}	8.56×10^{-2}	8.80×10^{-2}	8.04×10^{-2}	(3)
Gas-water mass transfer coefficient [s^{-1}]	calibrated¶	calibrated¶	calibrated¶	calibrated¶	(4)

¶ Calibrated seperately for each data set.

References: (1) *Weast* [1989]; (2) *this work*; (3) calculated according to *Wilke and Lee* [1955]; (4) *this work*;
§ *Dilling* [1977].

Legend (rotated):

- Equilibrium Model
- Kinetics Model: $\lambda_{gw} = 10^{-4}$ s^{-1}
- Kinetics Model: $\lambda_{gw} = 10^{-5}$ s^{-1}
- Kinetics Model: $\lambda_{gw} = 10^{-6}$ s^{-1}
- Kinetics Model: $\lambda_{gw} = 10^{-7}$ s^{-1}

Plot (rotated): Relative Concentration C / C_0 [-] versus Time [h]
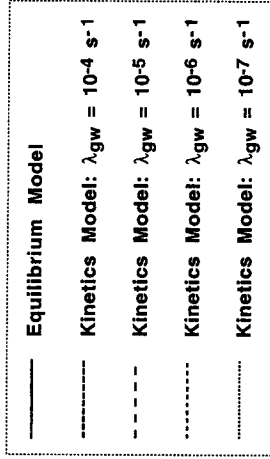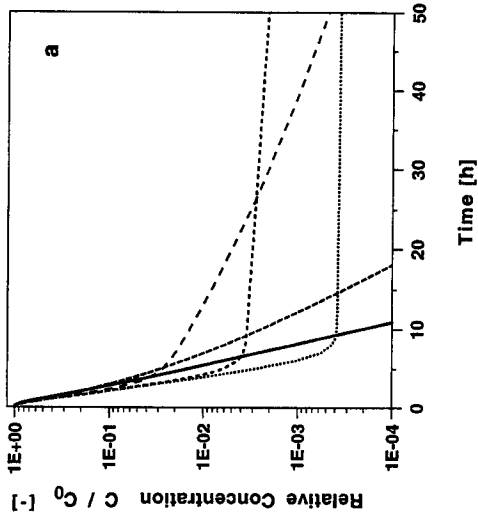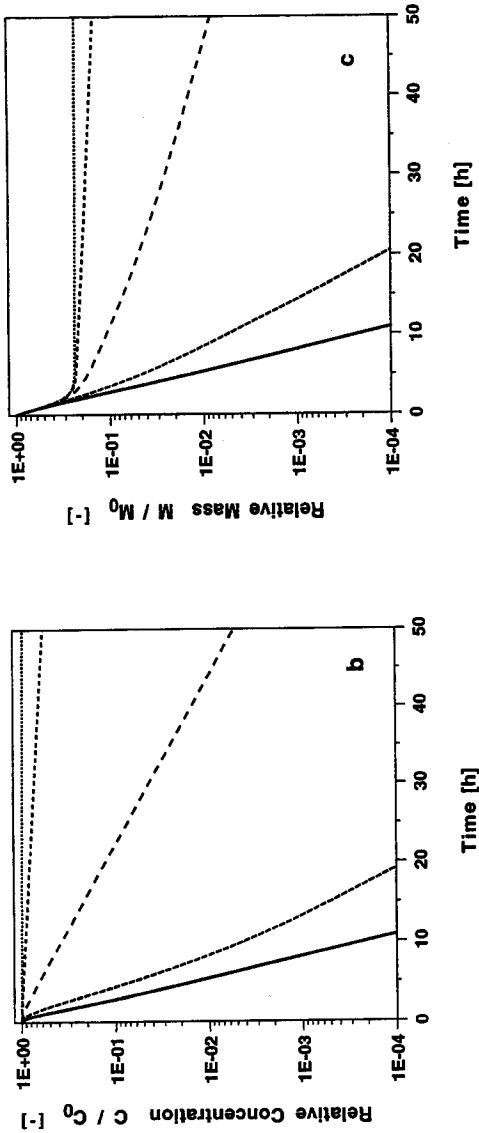
Figure 5.1 *Comparison of equilibrium model and kinetics model: a) Relative gas phase concentration. b) Relative water concentration. c) Relative mass in the domain. Simulations were done for trichloroethylene at sampling port SP 23 in experiment V1.*

time. The curves obtained with the equilibrium model for the three variables are
of identical shape (Figure 5.1a-c). This result means that gas concentrations can
be taken as a measure of VOC removal when the equilibrium model is
applicable.

The curves calculated with the kinetics model approached those of the
equilibrium model when the mass transfer coefficient was increased (Figure
5.1a-c). A mass transfer coefficient of 10^{-4} s^{-1} resulted in small differences
between time courses of relative gas concentration, water concentration, and
total mass. For small values of the mass transfer coefficient gas concentrations
showed a course that was markedly different from water concentrations and
total mass. Water concentrations decreased steadily for all values of λ_{gw}. In the
initial stage the mass in the domain decreased identically for all simulations. This
initial decrease in total mass corresponds to the mass which is present in the gas
phase at time zero. Mass courses calculated for small mass transfer coefficients
displayed a sharp transition as soon as the mass initially present in the gas phase
had been removed. The corresponding gas concentrations show a steep initial
decrease followed by a sharp transition and a long tail. The relative gas
concentrations in the tail (Figure 5.1a) are quite different from the
corresponding values of relative mass in the domain (Figure 5.1c). This
demonstrates that observation of a fast initial decrease in gas concentration
during SVE operations does not necessarily indicate a high mass removal rate
but also can signify a large deviation from equilibrium associated with a very
slow mass removal. Consequently, SVE experiments have to be observed for a
sufficiently long time period in order to determine the adequate model on the
basis of measured gas concentrations. This is shown in Figure 5.1a where the
equilibrium model and the kinetics simulation for λ_{gw} equal to 10^{-7} s^{-1} display
very similar curves of relative gas concentration for the first 5 to 10 h but then
diverged significantly from each other.

5.2 Sensitivity analysis

A sensitivity analysis was performed focussing on the intrinsic permeability and
the two parameters controlling mass transfer between gas and water in the two
mathematical models: the first-order mass transfer coefficient (kinetics model),
and the Henry's law constant (both models). The simulations presented in
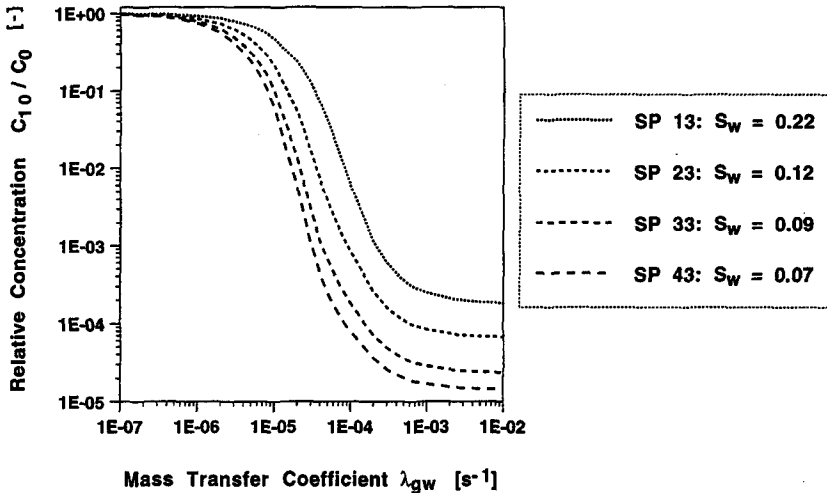
Figure 5.2   *Sensitivity of kinetics model with respect to mass transfer coefficient λ_{gw} at sampling ports (SP) with different water saturation S_w [-]. Sensitivity was assessed by means of relative water concentrations calculated for a simulation period of 10 h using the parameter values of the dry experiment (V1; cf. Table 5.1) and the physico-chemical data of 1,1,1-trichloroethane (cf. Table 5.2).*

Figure 5.1 demonstrate that model sensitivity should not be assessed on the basis of gas concentrations alone. Hence, water concentrations were used as a sensitivity measure. Sensitivity was assessed for a simulation period of 10 h using the parameter values of the dry experiment (V1; cf. Table 5.1) and the physico-chemical data of 1,1,1-trichloroethane (cf. Table 5.2).

The sensitivity of the kinetics model found with respect to the mass transfer coefficient is represented in Figure 5.2. Results are shown for locations of different water saturation. All curves display the same sigmoid shape in the double-logarithmic plot. Values of λ_{gw} below 10^{-6} s^{-1} resulted in relative water concentrations which were still close to unity after 10 h. In the range from 10^{-6} s^{-1} to 10^{-3} s^{-1} the kinetics model was most sensitive to changes of the mass transfer coefficient. Values of λ_{gw} above 10^{-3} s^{-1} gave nearly identical
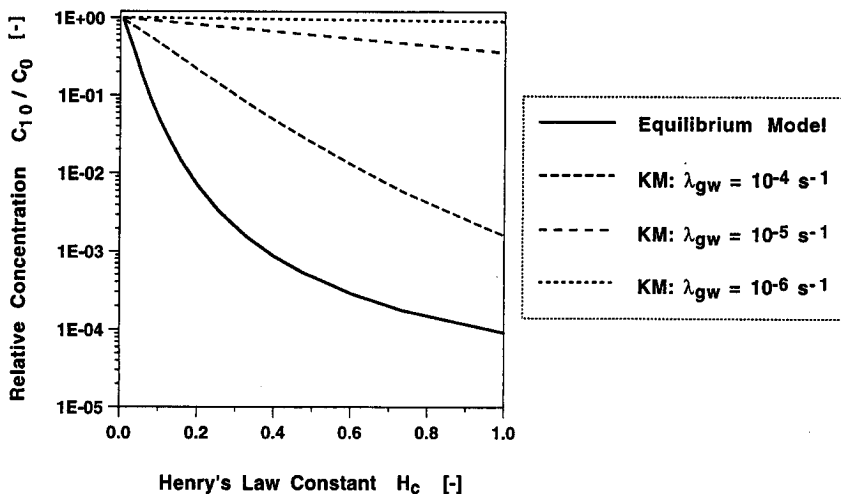
Figure 5.3   *Sensitivity of equilibrium model and kinetics model (KM) assuming different mass transfer coefficients λ_{gw} with respect to Henry's law constant at sampling port SP 13.   Sensitivity was assessed by means of relative water concentrations calculated for a simulation period of 10 h using the parameter values of the dry experiment (V1; cf. Table 5.1) and the physico-chemical data of 1,1,1-trichloroethane (cf. Table 5.2).*

concentrations. In this range the kinetics model approached the equilibrium model (cf. Figure 5.1). Differences in water concentration at locations with different water saturation were quite pronounced when the mass transfer coefficient exceeded 10^{-5} s^{-1}.

In the equilibrium model gas-water mass transfer is controlled by the Henry's law constant. Also in the kinetics model gas-water mass transfer depends on this parameter. The sensitivity of both models found with respect to the Henry's law constant is shown in Figure 5.3 where λ_{gw} was varied over three orders of magnitude (10^{-4} s^{-1} - 10^{-7} s^{-1}). The curves show that the equilibrium model was found to be most sensitive to the Henry's law constant. With this model water concentrations depended strongly on H_c in the range below 0.4. Sensitivity became quite small for larger values of the Henry's law
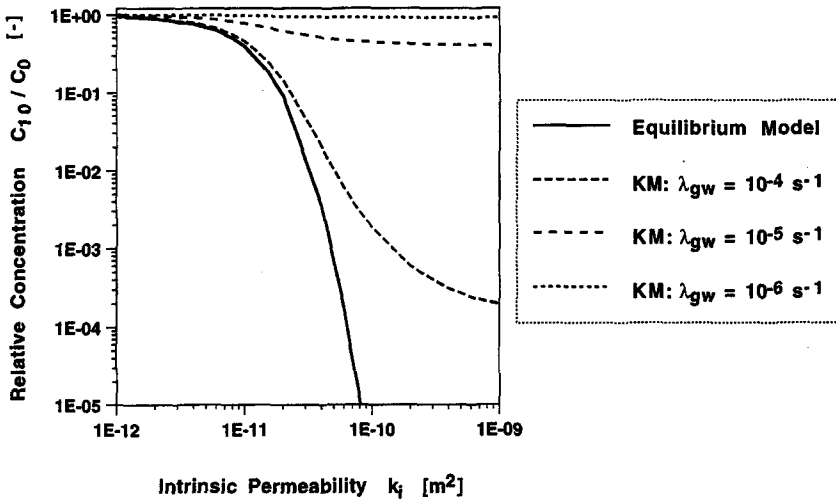
Figure 5.4   *Sensitivity of equilibrium model and kinetics model (KM) assuming different mass transfer coefficients λ_{gw} with respect to intrinsic permeability at sampling port SP 13. Sensitivity was assessed by means of relative water concentrations calculated for a simulation period of 10 h using the parameter values of the dry experiment (V1; cf. Table 5.1) and the physico-chemical data of 1,1,1-trichloroethane (cf. Table 5.2).*

constant. In the kinetics model the influence of H_c decreased as the mass transfer coefficient decreased. For values of λ_{gw} below 10^{-5} s^{-1} the influence of the Henry's law constant was quite small.

The sensitivity of both models found with respect to the intrinsic permeability is shown in Figure 5.4 where in the kinetics model λ_{gw} was varied over three orders of magnitude (10^{-4} s^{-1} - 10^{-7} s^{-1}). For values of the intrinsic permeability below 10^{-11} m^2 quite similar concentrations after 10 h were obtained with the equilibrium model and the kinetics model using different mass transfer coefficients. As the intrinsic permeability increased, the differences between the models increased. The equilibrium model was found to be very sensitive to the intrinsic permeability in the range above 10^{-11} m^2. A mass transfer coefficient of 10^{-6} s^{-1} in the kinetics model resulted in water concentrations which were close to unity after 10 h. As the mass transfer

coefficient increased the sensitivity of the kinetics model increased. If the intrinsic permeability exceeded certain values - which increased with increasing mass transfer coefficient - the sensitivity of the kinetics model decreased and the water concentrations after 10 h were nearly identical. According to Equation (4.4), the sensitivity to the intrinsic permeability also represents the sensitivity of the model to the function of relative gas permeability and to the applied gas pressure.

5.3   Modeling tank venting experiments - Model testing

The soil vapor extraction experiments presented in Section 3.3 showed the influence of water saturation, and of the Henry's law constants of the compounds on VOC removal in the absence of a liquid organic phase. 1,1,1-trichloroethane (1,1,1-TCA), trichloroethylene (TCE), and perchloroethylene (PCE) with dimensionless Henry's law constants of 0.73, 0.45, and 0.69, respectively, displayed very similar declines of relative gas concentration, whereas 1,1,2-trichloroethane (1,1,2-TCA) showed a markedly different behavior. A Henry's law constant of 0.09 was found for 1,1,2-TCA (cf. Section 3.2). Concentration data obtained from these soil venting experiments were used for testing the equilibrium model and the kinetics model.

Experiments V1 (dry), V2 (moist/slow), and V4 (moist/fast)

Figure 5.5 shows gas concentrations of the four VOCs measured at sampling port SP 13 (cf. Figure 2.3) during the moist/slow experiment (V2) and the corresponding numerical simulations using the equilibrium model. The calculated curves of relative concentration of 1,1,1-TCA, TCE, and PCE matched the experimental data obtained for the first 5 h. For later times the calculated concentrations continued to decrease steadily while the measured concentrations displayed a transition to a markedly slower decline. The large deviations between experimental data and equilibrium simulations were hardly detectable when a linear scale was used for the concentration axis. The equilibrium model failed to describe the concentrations measured for 1,1,2-TCA at any time when the independently determined value of the Henry's law
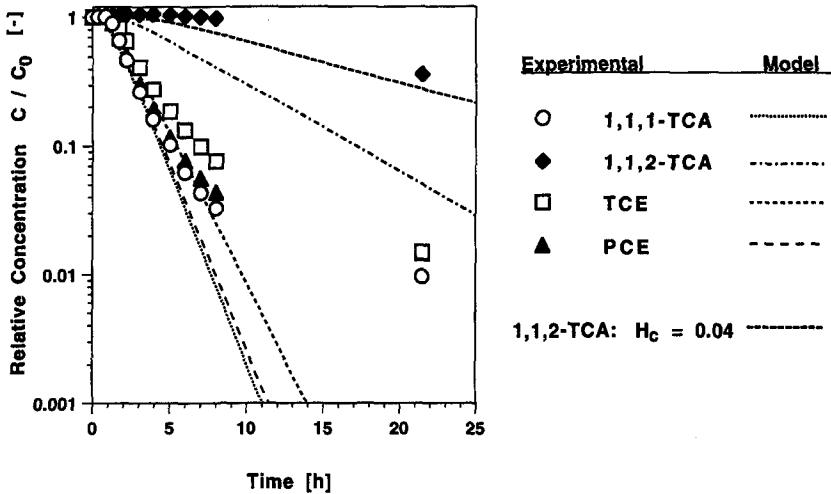
Figure 5.5   *Comparison of gas concentrations measured for 1,1,1-TCA, 1,1,2-TCA, TCE, and PCE at sampling port SP 13 during the moist/slow experiment (V2), and equilibrium simulations using the independently determined values of the Henry's law constants. In addition, the equilibrium simulation using a value of 0.04 as Henry's law constant for 1,1,2-TCA is shown. Note coincidence of last measurements for TCE and PCE.*

constant was used. The kinetics model with mass transfer coefficients λ_{gw} in the range from 10^{-7} s^{-1} to 10^{-3} s^{-1} failed to match the data better. For comparison, the literature value of 0.04 [*Dilling*, 1977] was used as Henry's law constant for 1,1,2-TCA in the equilibrium model. With this choice the model described the data quite well for the whole duration of the experiment (Figure 5.5). Similar results as presented in Figure 5.5 were obtained also for other sampling ports in the dry experiment (V1) and the moist/slow experiment (V2). The equilibrium model matched the early time concentrations of 1,1,1-TCA, TCE, and PCE but failed to describe them for late times. Concentrations of 1,1,2-TCA were described quite well by the equilibrium model for the entire observation periods when a value of the Henry's law constant of 0.04 was used.
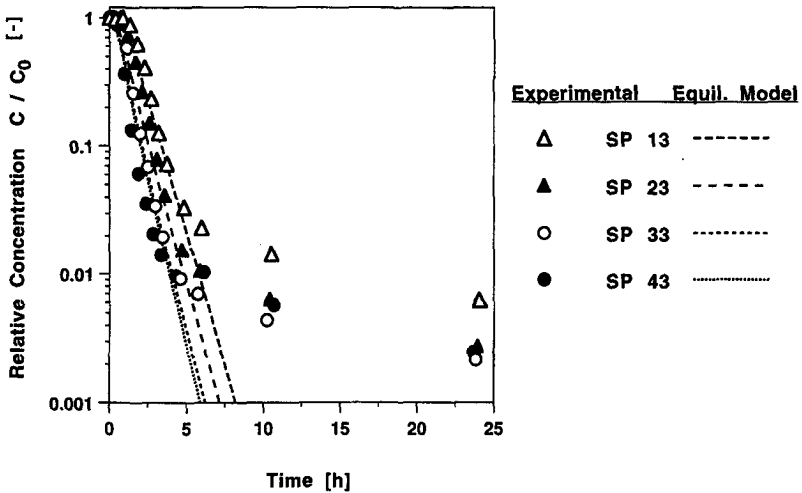
Figure 5.6   *Comparison of experimental gas concentrations obtained for 1,1,1-trichloroethane at four sampling ports (SP) during the dry experiment (V1) and equilibrium simulations.*

Figure 5.6 shows a comparison of experimental data obtained for 1,1,1-TCA at four sampling ports during the dry experiment (V1) and theoretical curves calculated with the equilibrium model. For early times the equilibrium model matched the experimental data and predicted the effect of different water saturations quite well. It failed to describe the tailing of the concentration courses. Nevertheless, the agreement between experiment and model at each location for early times indicates that in this period mass transfer between gas and water could be described by means of the local equilibrium assumption. Obviously, this was not true for later stages of the experiment. The equilibrium model also failed to describe the amount of mass which was retained in the tank at the end of the experiment.

In the kinetics model mass transfer between gas and water is controlled by the first-order mass transfer coefficient. In this study the values of the mass transfer coefficient λ_{gw} could not be determined independently. For each set of
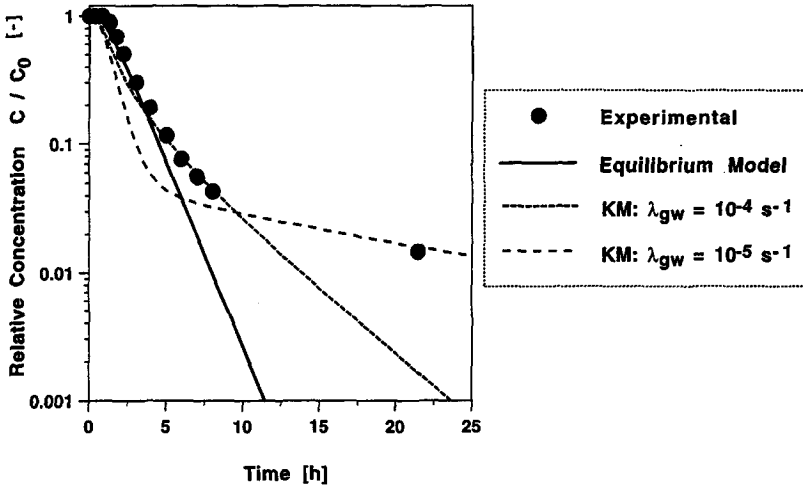
Figure 5.7 *Comparison of experimental gas concentrations obtained for perchloroethylene at sampling port SP 13 during the moist/slow experiment (V2), and simulations using the equilibrium model and the kinetics model assuming two different mass transfer coefficients λ_{gw}.*

data obtained in the dry experiment (V1) and the moist/slow experiment (V2) the mass transfer coefficient was calibrated by curve-fitting with a precision of one significant digit. For some data sets it was not possible to match all data by means of a single valued mass transfer coefficient. Figure 5.7 shows gas concentrations measured for PCE at sampling port SP 13 during the moist/slow experiment (V2) and corresponding simulations using the equilibrium model and the kinetics model. Simulations with the kinetics model were done with two different values of the mass transfer coefficient (10^{-4} s^{-1} and 10^{-5} s^{-1}). The equilibrium model matched the early time data. Concentrations measured in the period from 5 h to 10 h were well represented by the kinetics model using a mass transfer coefficient equal to 10^{-4} s^{-1}. A value of 10^{-5} s^{-1} matched the concentrations observed in the period from 10 h to 25 h but failed to describe the early time data.

In section 3.3 it was hypothesized that the local nonequilibrium in the experiments most probably was due to diffusion within the interparticle water,

especially within the water in the wedges between the sand grains. *Rao et al.* [1980] investigated mass transfer between mobile and immobile soil-water regions. They showed that for spherical aggregates the mass transfer coefficient of the first-order kinetics model cannot be expected to be constant, because the geometry of the stagnant region and the concentration gradients of the solute in this domain are not accounted for by the first-order kinetics approach. These authors found that the mass transfer coefficient decreased with time and approached a constant value for large times. For certain geometries diffusion from nonspherical aggregates can be approximated by diffusion in equivalent spheres [*Rao et al.*, 1982]. This suggests that if the diffusion process in the interparticle water of the sand packing investigated in the present study is modeled by means of first order kinetics, then the mass transfer coefficient is not constant but approaches a limiting value for large times. Therefore, values of the mass transfer coefficient were selected which matched the late time data especially well taking into account that simulations and data possibly coincided less for early times. Calibrations were done for each data set (obtained at one sampling port) separately using a uniform mass transfer coefficient for the whole domain. Using the mass transfer coefficients calibrated at the respective sampling ports and interpolated values of λ_{gw} at the nodes between the sampling ports, simulations were carried out in which λ_{gw} was varied with water saturation. For all sampling ports the difference between the curve calculated for a water saturation-dependent mass transfer coefficient and the curve obtained for a uniform mass transfer coefficient were negligible.

The same data which are compared to the equilibrium model in Figure 5.6 are presented again in Figure 5.8 and compared to the kinetics model. This model in general described the experimental data well if calibrated mass transfer coefficients were used. For sampling ports SP 13 and SP 23 there was a slight deviation between model and experimental data for early times, whereas for SP 43 the calculated curve did not match the concentrations observed at late times. In the latter case no better calibration with regard to the late time data was obtained. The mass transfer coefficient had to be decreased as the water saturation decreased. Calibrated values of λ_{gw} range from 6×10^{-6} s^{-1} at sampling port SP 13 to 2×10^{-6} s^{-1} at SP 33 and SP 43. The mass retained in the tank at the end of the experiment was matched when a value of 6×10^{-6} s^{-1} was used. As mentioned above, data obtained for 1,1,2-TCA were described quite well by the equilibrium model. In the range of large mass transfer
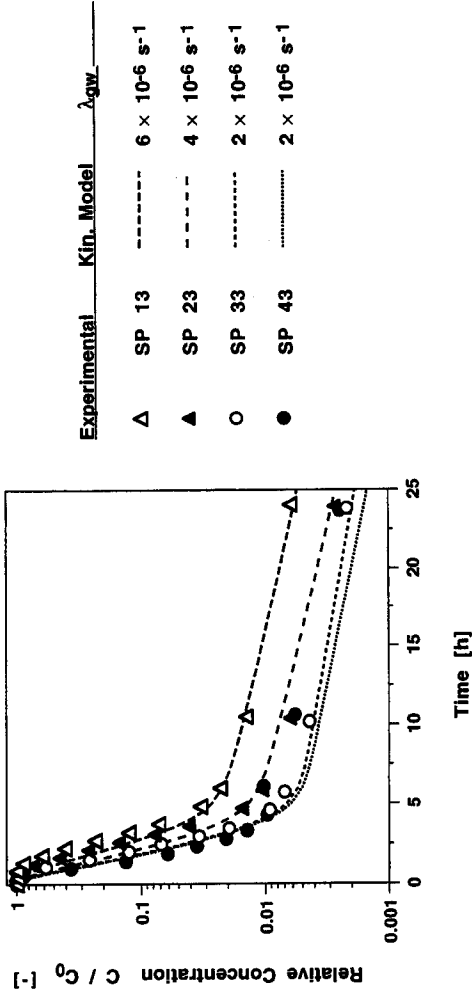
Figure 5.8 *Comparison of experimental gas concentrations obtained for 1,1,1-trichloroethane at four sampling ports (SP) during the dry experiment (VI) and simulations obtained with the kinetics model using calibrated mass transfer coefficients λ_{gw}.*
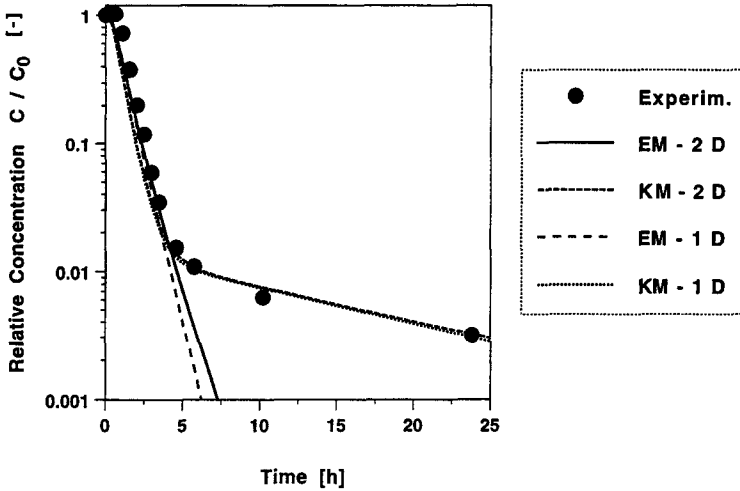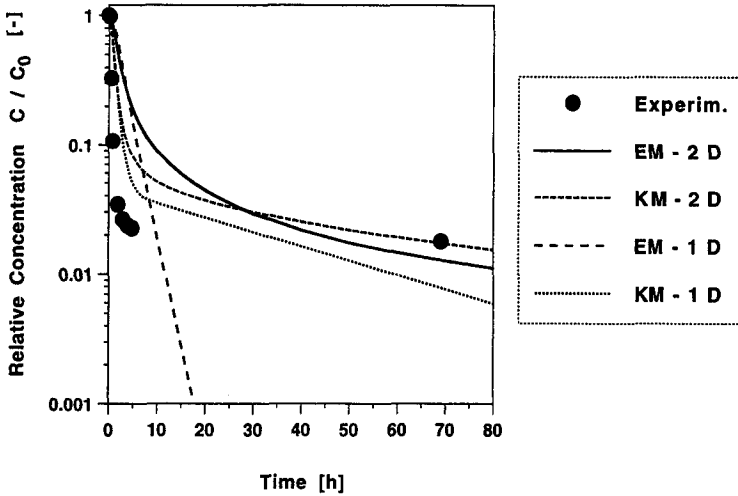
Figure 5.9   *Comparison of experimental gas concentrations obtained for trichloroethylene at sampling port SP 33 during the dry experiment (V1), and one- and two-dimensional simulations obtained with both the equilibrium model (EM) and the kinetics model (KM; $\lambda_{gw} = 2 \times 10^{-6} s^{-1}$).*

coefficients the kinetics model is very insensitive to changes in this parameter (cf. Figure 5.2). For 1,1,2-TCA values for the mass transfer coefficient were taken which matched the amount of mass retained in the tank at the end of the experiment.

The experimental results presented in Section 3.3 showed that gas concentrations decreased more slowly at sampling ports with high water saturation than at locations with low water saturation. This may suggest that upward diffusion within the gas phase was the main factor causing the observed tailing of gas concentrations. In Figure 5.9 the two-dimensional simulations obtained with the equilibrium model and the kinetics model for trichloroethylene at SP 33 in the dry (V1) experiment are compared to so called "one-dimensional simulations" and to the experimental data. In the one-dimensional simulations the water saturation at the sampling port under consideration was taken to represent a uniform value all over the two-
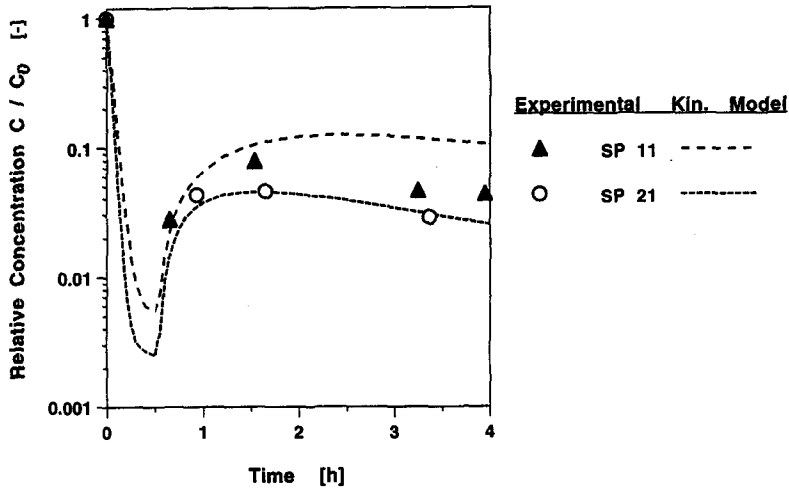
Figure 5.10 *Comparison of simulations obtained with the kinetics model ($\lambda_{gw} = 5 \times 10^{-5} \ s^{-1}$) and experimental gas concentrations obtained for perchloroethylene at two sampling ports (SP) during the moist/fast experiment (V4). Gas flow was reduced from 6.6 to 1.0 L min^{-1} after 0.5 h. Prior to flow reduction concentrations were fallen below the detection limit.*

dimensional domain. Only the kinetics model described the data well, and the difference between the one- and the two-dimensional kinetics simulation was quite small. Also for the equilibrium model the difference between one- and two-dimensional calculation was small but these simulations only matched the experimental data obtained during the first 5h. Similar results were obtained for other sampling ports in the dry experiment (V1) and the moist/slow experiment (V2). It can be concluded that in these two experiments transport of VOCs occured mainly in the direction of gas flow (horizontal-longitudinal), and that the tailing of gas concentrations observed in these experiments was not due to upward diffusion within the gas phase. The comparison of gas concentrations measured in experiments V1 and V2 and numerical simulations obtained with the equilibrium model and the kinetics model is completed in Figures A.4 - A.10 in the Appendix.

In the moist/fast experiment (V4) the initial rate of gas flow was rather high, and gas concentrations quickly fell below the detection limits. Then, after 0.5 h, gas flow was reduced from 6.6 L min^{-1} to 1.0 L min^{-1}. The decrease in flow rate resulted in a temporary rise of gas concentrations. The kinetics model described the rise of concentration at sampling port SP 21 as well as the following decrease quite well using a mass transfer coefficient of 5×10^{-5} s^{-1} (Figure 5.10). The model underestimated the concentration decrease at sampling port SP 11 in the period from 2 h to 4 h but reproduced the general shape of the concentration curve well. The general coincidence between kinetics simulations and data indicates that the fast concentration rises observed after flow reduction were due to local nonequilibrium between gas phase and aqueous phase.

Experiment V3 (wet)

Figure 5.11 shows a comparison of experimental data obtained for TCE in the wet experiment (V3) and the two models. A mass transfer coefficient of 1×10^{-5} s^{-1} was used in the kinetics model. In this experiment at sampling port SP 22 gas flow was zero, and thus, VOC removal was entirely controlled by diffusion into the region where gas flow occured. The equilibrium simulation gave concentrations somewhat higher than the experimental data obtained at SP 22, whereas the kinetics model matched these data quite well (Figure 5.11). Also at the other two sampling ports the kinetics model described the data better than the equilibrium model but the agreement with the measured concentrations was not very good in neither case. No better fits for SP 32 and SP 42 were obtained with other mass transfer coefficients in the kinetics model. The mass of TCE retained in the tank at the end of the experiment was better approximated by the equilibrium model. Similar results as for TCE were also obtained for the other compounds (cf. Figures A.11 - A.13 in the Appendix).

The wide variation of water saturation and average linear velocity must have resulted in completely different transport regimes in the tank during the wet experiment (V3). The results obtained from experiments V1 (dry) and V2 (moist/slow) suggest that in the zone of low water saturation and high linear gas velocity VOC removal quickly became a nonequilibrium process. With increasing water saturation gas velocities decreased, and the upward diffusive
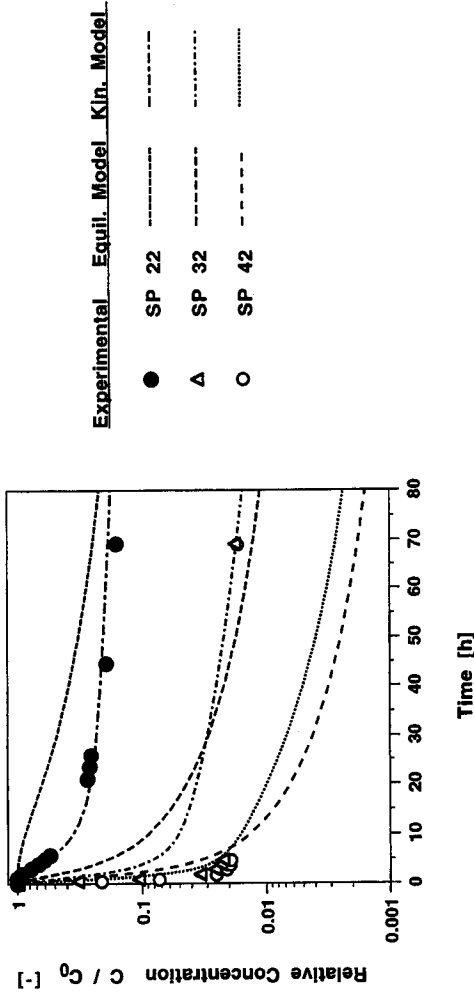
Figure 5.11 *Comparison of equilibrium model, kinetics model ($\lambda_{gw} = 10^{-5}\ s^{-1}$), and experimental gas concentrations obtained for trichloroethylene at different sampling ports (SP) during the wet experiment (V3). Note coincidence of last measurements at SP 32 and SP 42.*

Figure 5.12 *Comparison of experimental gas concentrations obtained for trichloroethylene at sampling port SP 33 during the wet experiment (V3), and one- and two-dimensional simulations obtained with both the equilibrium model (EM) and the kinetics model (KM; $\lambda_{gw} = 1 \times 10^{-5}\ s^{-1}$).*

flux increased. The role of upward diffusion is demonstrated by Figure 5.12. In this graph the two-dimensional simulations obtained with the equilibrium model and the kinetics model for trichloroethylene at SP 32 in the wet experiment (V3) are compared to one-dimensional simulations and to the experimental data. The two-dimensional simulations obtained with the equilibrium model and the kinetics model are quite similar. The one-dimensional simulation obtained with the kinetics model differed much more from the two-dimensional calculation than it did in the dry experiment (V1; cf. Figure 5.9). The one-dimensional simulation obtained with the equilibrium model differs markedly from the two-dimensional calculation which described the experimental data more or less as well as the kinetics model. This result demonstrates that in the wet experiment (V3) transport of VOCs occured not only in the direction of gas flow (horizontal-longitudinal) but also by diffusion in the vertical direction. As a consequence of the different transport regimes, spatially variable mass transfer coefficients have to be used to model this experiment correctly. As long as mass

transfer coefficients cannot be determined independently, inverse modeling has to be applied to obtain these parameters, rendering the calibration problem much more complex.

6

ASSESSMENT OF NONEQUILIBRIUM

Various concepts have been used to assess the validity of the local equilibrium assumption. *Valocchi* [1985] and *Parker and Valocchi* [1986] based their analysis on the comparison of temporal moments of solute breakthrough curves. *Jennings and Kirkner* [1984] expressed the validity of the LEA in terms of the Damköhler I number [*Damköhler*, 1936]. *Bahr and Rubin* [1987] developed the procedure of separation of the kinetically influenced term (SKIT). By means of SKIT, the prefix denominator P_D is derived, which provides an alternative measure for nonequilibrium. On the basis of numerical simulations *Bahr and Rubin* [1987] concluded that the magnitude of the kinetically influenced term as a whole is controlled by the magnitude of the prefix factor with denominator P_D.

6.1 Derivation of the prefix denominator P_D for gas-water mass transfer

The procedure of deriving P_D for a given model is given in detail by *Bahr and Rubin* [1987]. Equivalent dimensionless formulations of the equilibrium model and the kinetics model have to be derived and compared with each other to identify the additional term in the nonequilibrium model which is called the kinetically influenced term. The transport equation representing the equilibrium model in dimensionless form is:

$$\frac{\partial C_g'}{\partial T} = \frac{\partial}{\partial X_i}\left(\frac{1}{Pe_{ij}}\frac{\partial C_g'}{\partial X_j}\right) - V_i\frac{\partial C_g'}{\partial X_i} \equiv L'(C_g') \qquad (6.1)$$

where $L'(C_g')$ denotes the dimensionless differential operator representing the convective and dispersive terms, and

$$C_g' = \frac{C_g}{C_0} \qquad T = \frac{v_x\, t}{R\, L_x} \qquad X_i = \frac{x_i}{L_x} \qquad Pe_{ij} = \frac{L_x\, v_x}{D_{ij}} \qquad V_i = \frac{v_i}{v_x} \qquad \text{(6.2a-e)}$$

where C_g' is the relative gas concentration, T is dimensionless time, L_x is a reference length in x-direction [L], the X_i are relative distances in x- and z-direction normalized by L_x, Pe_{ij} denotes the Peclet numbers, and the V_i are relative velocities normalized by the velocity component in x-direction. In order to derive the corresponding formulation representing the kinetics model, (4.23) is rearranged to obtain an expression for C_w:

$$C_w = \frac{1}{\lambda_{gw}\, H_c}\left[\frac{\partial C_g}{\partial t} - \frac{1}{\theta_g} L(C_g)\right] + \frac{1}{H_c} C_g \qquad \text{(6.3)}$$

Differentiating (6.3) with respect to time gives:

$$\frac{\partial C_w}{\partial t} = \frac{1}{\lambda_{gw}\, H_c}\, \frac{\partial}{\partial t}\left[\frac{\partial C_g}{\partial t} - \frac{1}{\theta_g} L(C_g)\right] + \frac{1}{H_c}\, \frac{\partial C_g}{\partial t} \qquad \text{(6.4)}$$

This expression is substituted into (4.18). Using the differential operator instead of the convective and dispersive terms, and rearranging yields:

$$\frac{\partial C_g}{\partial t} = \frac{1}{\theta_g\, R} L(C_g) - \frac{1}{\lambda_{gw}\, R\, \dfrac{H_c\, \theta_g}{\theta_w}}\, \frac{\partial}{\partial t}\left[\frac{\partial C_g}{\partial t} - \frac{1}{\theta_g} L(C_g)\right] \qquad \text{(6.5)}$$

In dimensionless form (6.5) becomes:

$$\frac{\partial C_g'}{\partial T} = L'(C_g') - \frac{1}{\omega\, R\, \dfrac{H_c\, \theta_g}{\theta_w}}\, \frac{\partial}{\partial T}\left[\frac{1}{R}\, \frac{\partial C_g'}{\partial T} - L'(C_g')\right] \qquad \text{(6.6)}$$

where ω is the Damköhler I number defined as:

$$\omega = \frac{\lambda_{gw}\, L_x}{v_x} \qquad \text{(6.7)}$$

The second term on the right hand side of (6.6) does not appear in (6.1) and thus represents the kinetically influenced term. The reciprocal of the factor in front of the dimensionless time derivative of the kinetically influenced term is the prefix denominator P_D for gas-water mass transfer in the kinetics model:

$$P_D = \omega R \frac{H_c \, \theta_g}{\theta_w} \tag{6.8}$$

6.2 Evaluation of nonequilibrium using ω and P_D - Nonequilibrium as a function of dimensionless time

For the 32 data sets obtained in the dry experiment (V1) and the moist/slow experiment (V2) the values of ω and P_D were calculated according to (6.7) and (6.8), respectively, using the calibrated mass transfer coefficients. Linear velocities in x-direction, v_x, were approximated by average linear velocities v which were calculated using Equation (3.8).

The largest calculated values of ω and P_D were in the order of 4. The corresponding data, all obtained for 1,1,2-TCA, could be described by the equilibrium model. The largest values for which the corresponding data could not be described by the equilibrium model at all times were in the order of 0.4. *Jennings and Kirkner* [1984], *Valocchi* [1985], and *Bahr and Rubin* [1987] investigated the validity of the local equilibrium assumption (LEA) for modeling sorption and complexation processes. These authors concluded that the LEA is applicable if the Damköhler I number exceeds 100. *Jennings and Kirkner* [1984] obtained reasonably good approximations of the LEA for values of w greater than 10. For values below 1 the LEA led to large simulation errors. Thus, the results found in the present study agree quite well with the findings of *Jennings and Kirkner* [1984].

Bahr and Rubin [1987] reported that equilibrium transport can be assumed for values of the dimensionless prefix denominator P_D in the order of 100 or greater. The values of P_D for which transport has been found to be close to local equilibrium conditions in the present study are one order of magnitude smaller and suggest that already for P_D values of 10 the LEA may be a good approximation. In the following the prefix denominator is used as a measure of nonequilibrium as it considers capacity factors representing the varying

experimental conditions (water saturation) and physico-chemical properties of the compounds (Henry's law constant, solid-water distribution coefficient) in addition to gas velocitiy and gas-water mass transfer coefficient.

In Section 3.3 it has been shown that the concentration courses of the 32 data sets obtained in the dry experiment (V1) and the moist/slow experiment (V2) could be scaled quite well to a dimensionless time T (cf. Equation 3.9). The last measurements C_E/C_0 of the 32 concentration courses plotted as a function of the corresponding values of dimensionless time T_E were found to represent the function between relative concentration and dimensionless time quite well (cf. Figure 5.12). In Figure 6.1a mass transfer coefficients λ_{gw} calibrated to the 32 data sets are plotted plotted as a function of T_E. The values obtained for 1,1,2-TCA lie close together because the mass transfer coefficients were determined by matching the remaining mass at the end of the experiment and therefore are identical for all sampling ports within a given experiment. The calibrated values of the mass transfer coefficient decreased with T_E and approached a limiting value of about 10^{-6} s^{-1}. This finding which is based on all 32 data sets is in agreement with the previous conclusion (cf. Figure 5.7) that the gas-water mass transfer coefficient in the first-order kinetics model is not a constant but approaches a limiting value for large times. Mass transfer coefficients presented in Figure 6.1a were used to calculate values of P_D in order to assess the degree of nonequilibrium at the end of the experiments. These values are shown in Figure 6.1b. They decrease with dimensionless time and approach a limiting value of about 10^{-2}. Thus, it can be expected that for large times not only the transport of 1,1,1-TCA, TCE, and PCE but also the removal of 1,1,2-TCA would have shown nonequilibrium behavior.
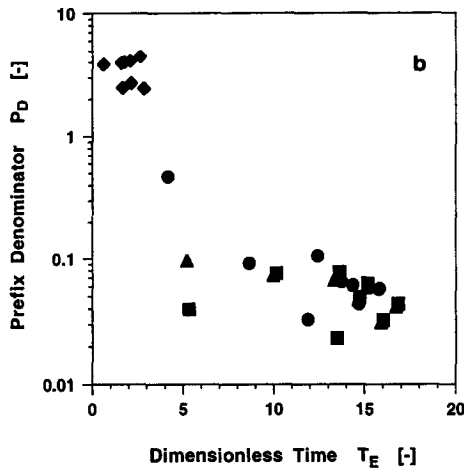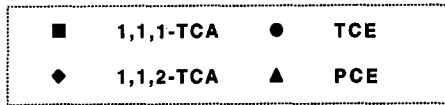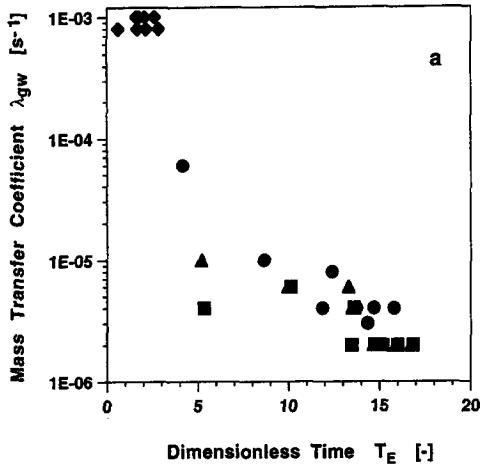
Figure 6.1 *Degree of nonequilibrium at the end of experiments V1 (dry) and V2 (moist/slow) as a function of corresponding dimensionless time T_E for 1,1,1-trichloroethane (1,1,1-TCA), 1,1,2-trichloroethane (1,1,2-TCA), trichloroethylene (TCE), and perchloroethylene (PCE): a) Calibrated mass transfer coefficient λ_{gw}. b) Prefix denominator P_D.*

7

CONCLUSIONS

The experimental results showed the influence of water saturation and the compounds' Henry's law constants on the removal of VOCs by soil vapor extraction in the absence of a liquid organic phase. Gas concentrations decreased more slowly at locations with high water saturation and for compounds with small Henry's law constant. Relative permeability of gas was not detectable at water saturations above 0.58 and 0.66 attained by drying and wetting, respectively. In the region where gas flow was zero VOC removal was limited by diffusion into the region where gas flow occured. As a consequence, mass removal from domains of high water saturation proceeded quite slowly. Thus, knowledge of the gas permeability function is of major importance in modeling soil vapor extraction operations.

Courses of relative gas concentration observed in experiments conducted at low water saturation were found to be a function of dimensionless time. The tailing suggested that nonequilibrium conditions prevailed in the experiments for large dimensionless times. As the investigated compounds were not found to adsorb on the soil material, volatilization from the aqueous phase was the key process for VOC removal. The water formed films on the nonporous particles, and wedges between them. It was concluded that the observed tailing of gas concentrations was the result of slow mass transfer from the wedges into the gas due to the limiting effect of diffusion within the aqueous phase. Hence, solely diffusion in interparticle water can cause tailing of gas concentrations during soil vapor extraction.

It can be concluded that even in soil materials which are homogeneous, low in sorptive capacity, without secondary porosity, and at low water saturation SVE operations can be affected by local nonequilibrium conditions. This would mean that even at such sites the removal of contaminants could not be enhanced markedly by increasing the flow rate, and that other strategies

have to be considered to increase the efficiency of the venting operation, e.g. pulsed pumping or injection of heated air.

In order to examine the hypothesis of kinetically limited volatilization, two gas flow and transport models were tested which differed in the description of mass transfer from the aqueous phase into the gas phase: the local equilibrium assumption and first-order kinetics. The equilibrium model matched the early time data obtained for compounds with large Henry's law constant in experiments conducted at low water saturation but failed to describe the observed tailing. The kinetics model described these experimental data quite well if calibrated mass transfer coefficients were used. The equilibrium model matched data obtained for a compound with small Henry's law constant for all times.

For some data sets the gas-water mass transfer coefficient in the kinetics model had to be decreased with time in order to match the data obtained from all stages of the experiments. The degree of nonequilibrium in the experiments was assessed by means of the Damköhler I number ω and the prefix denominator P_D. The degree of nonequilibrium increased with dimensionless time. Thus, it can be expected that also the removal of compounds with small Henry's law constant from the aqueous phase becomes a nonequilibrium process at large dimensionless times.

Data obtained in an experiment conducted at high water saturation could not be described by the equilibrium model. Modeling this experiment with the kinetics model rendered the calibration problem much more complex compared to experiments conducted at low water saturation, because inverse modeling is required unless mass transfer coefficients between gas and water can be estimated independently.

The fact that the local equilibrium assumption (LEA) failed to apply in the case of a nonsorbing homogeneous medium at gas-flow rates which are typical for SVE field operations means that it is in general not appropriate for modeling VOC removal from the aqueous phase in soil vapor extraction operations.

APPENDIX

In part 1 of the Appendix the concentrations of perchloroethylene and 1,1,1-trichloroethane measured during experiments V1 (dry), V2 (moist/slow), and V3 (wet) are presented in graphical form. In part 2 experimental results are compared with numerical simulations obtained with both the equilibrium model and the kinetics model.

Part 1

In Section 3.3 the concentrations measured for trichloroethylene and 1,1,2-trichloroethane during experiments V1 (dry), V2 (moist/slow), and V3 (wet) were presented. In these experiments perchloroethylene and 1,1,1-trichloroethane showed quite similar concentration courses as trichloroethylene. In the following three figures the concentrations measured for perchloroethylene and 1,1,1-trichloroethane are presented.
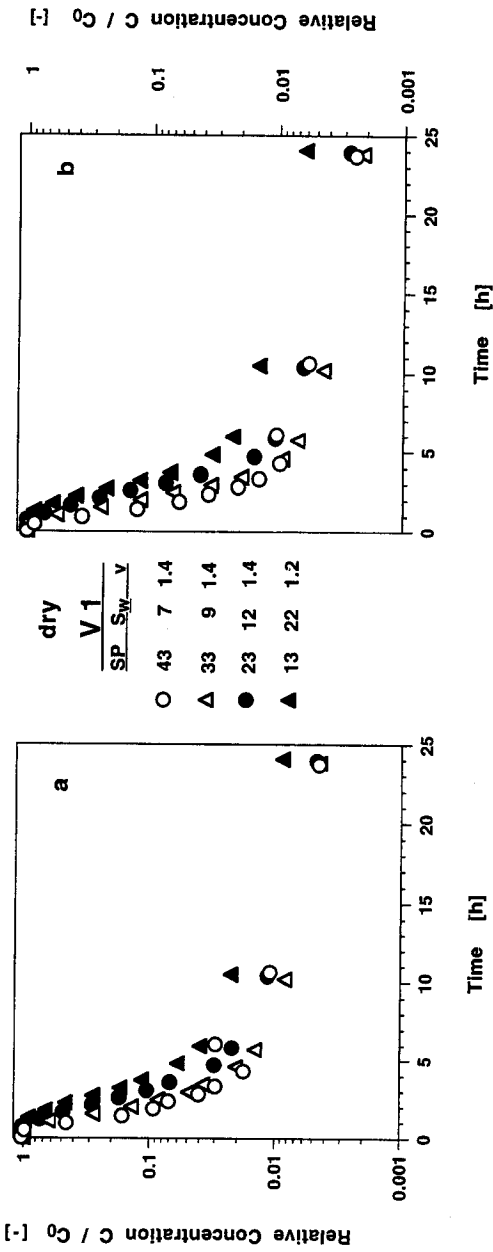
Figure A.1 *Relative gas concentrations of perchloroethylene (a) and 1,1,1-trichloroethane (b) at several sampling ports (SP) during the dry soil vapor extraction experiment (V1). Water saturation S_w [%] and average linear velocity v [$\times 10^{-2}$ cm s^{-1}] at each sampling port are given in the legend.*
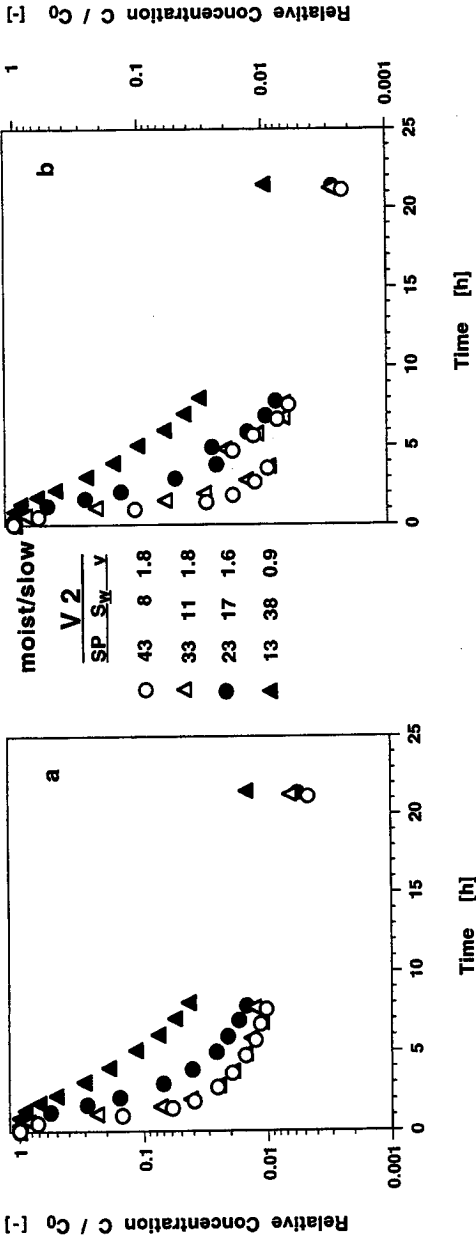
Figure A.2 *Relative gas concentrations of perchloroethylene (a) and 1,1,1-trichloroethane (b) at several sampling ports (SP) during the moist/slow soil vapor extraction experiment (V2). Water saturation S_w [%] and average linear velocity v [$\times 10^{-2}$ cm s^{-1}] at each sampling port are given in the legend.*
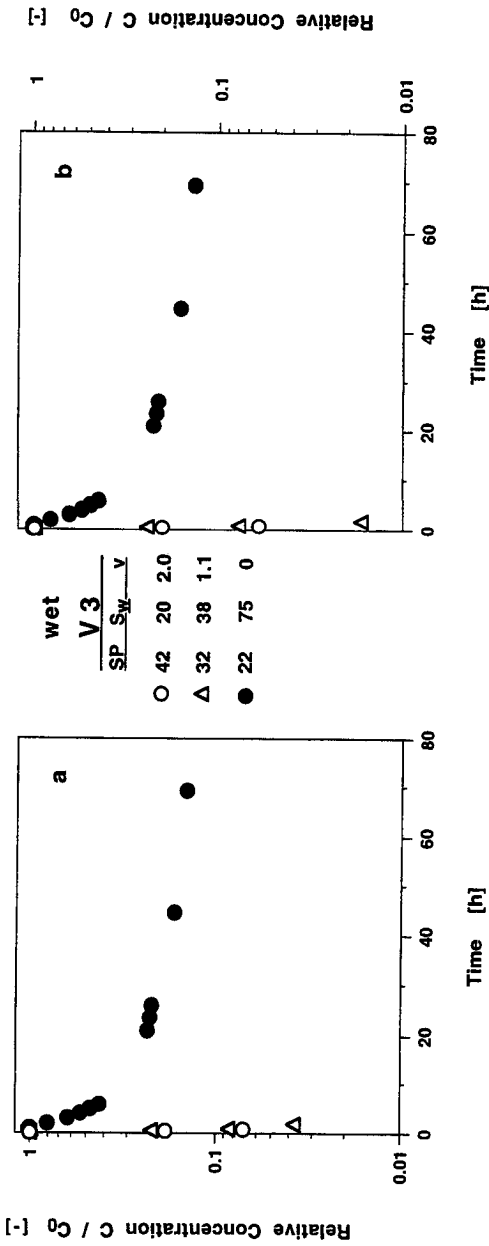
Figure A.3 *Relative gas concentrations of perchloroethylene (a) and 1,1,1-trichloroethane (b) at several sampling ports (SP) during the wet soil vapor extraction experiment (V3). Water saturation S_w [%] and average linear velocity v [$\times 10^{-2}$ cm s^{-1}] at each sampling port are given in the legend.*

Part 2

In the following figures the concentrations measured for 1,1,1-trichloroethane, 1,1,2-trichloroethane, trichloroethylene, and perchloroethylene during experiments V1 (dry), V2 (moist/slow), and V3 (wet) are compared to numerical simulations obtained with both the equilibrium model and the kinetics model (cf. Chapter 4). In Section 5.3 the concentrations measured for 1,1,1-trichloroethane during the dry experiment (V1) were compared to the equilibrium simulations (cf. Figure 5. 6) and to the kinetics simulations (cf. Figure 5. 8). In Figure 5.11 the concentrations measured for trichloroethylene during the wet experiment (V3) were compared to simulations obtained with both models.

Figure A.4 *Comparison of experimental gas concentrations obtained for 1,1,2-trichloroethane at four sampling ports (SP) during the dry experiment (V1) and simulations ($H_c = 0.04$) obtained with a) the equilibrium model and b) the kinetics model (KM) using calibrated mass transfer coefficients λ_{gw}.*

Figure A.5 *Comparison of experimental gas concentrations obtained for trichloroethylene at four sampling ports (SP) during the dry experiment (V1) and simulations obtained with a) the equilibrium model and b) the kinetics model (KM) using calibrated mass transfer coefficients λ_{gw}.*

Figure A.6 *Comparison of experimental gas concentrations obtained for perchloroethylene at four sampling ports (SP) during the dry experiment (V1) and simulations obtained with a) the equilibrium model and b) the kinetics model (KM) using calibrated mass transfer coefficients λ_{gw}.*

Figure   A.7 *Comparison of experimental gas concentrations obtained for 1,1,1-trichloroethane at four sampling ports (SP) during the moist/slow experiment (V2) and simulations obtained with a) the equilibrium model and b) the kinetics model (KM) using calibrated mass transfer coefficients λ_{gw}.*
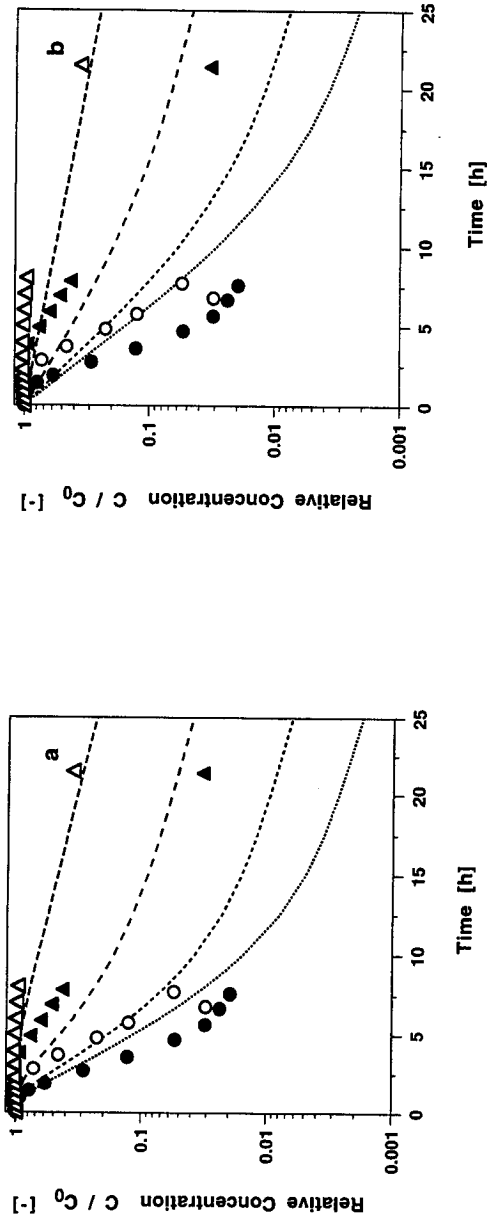
Figure A.8 *Comparison of experimental gas concentrations obtained for 1,1,2-trichloroethane at four sampling ports (SP) during the moist/slow experiment (V2) and simulations ($H_c = 0.04$) obtained with a) the equilibrium model and b) the kinetics model (KM) using calibrated mass transfer coefficients λ_{gw}.*
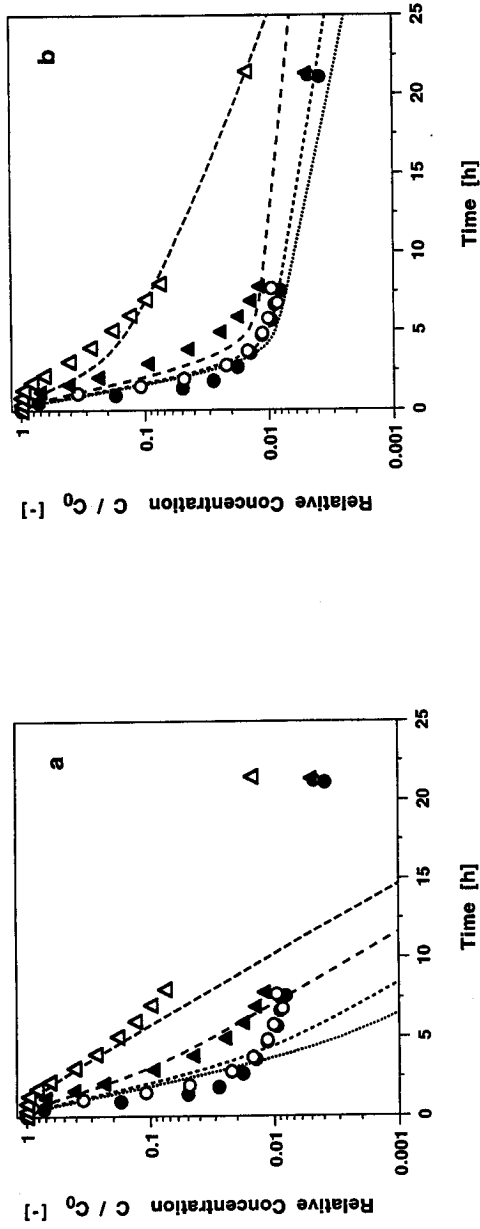
Figure A.9 *Comparison of experimental gas concentrations obtained for trichloroethylene at four sampling ports (SP) during the moist/slow experiment (V2) and simulations obtained with a) the equilibrium model and b) the kinetics model (KM) using calibrated mass transfer coefficients λ_{gw}.*
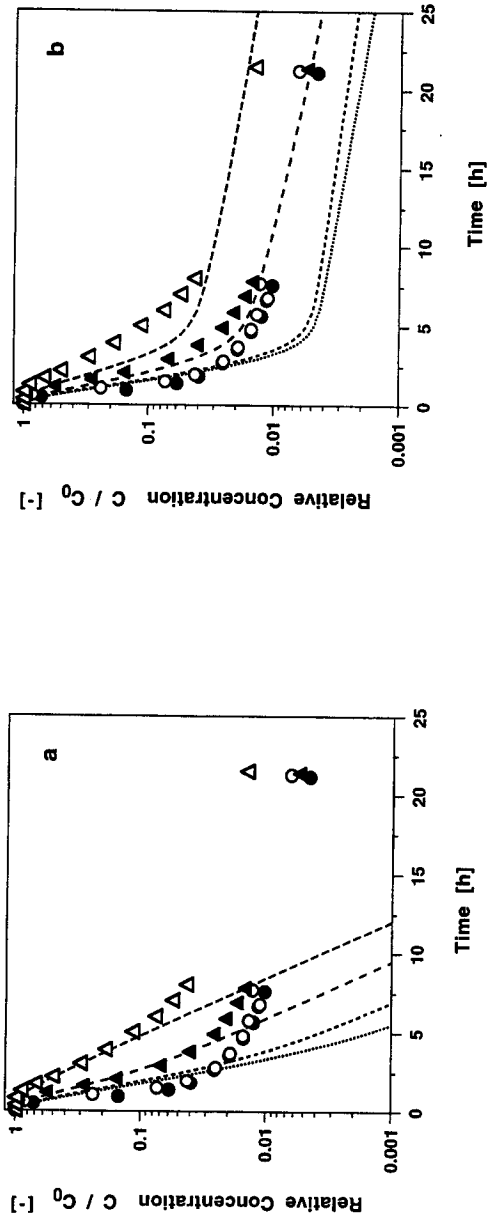
Figure A.10 *Comparison of experimental gas concentrations obtained for perchloroethylene at four sampling ports (SP) during the moist/slow experiment (V2) and simulations obtained with a) the equilibrium model and b) the kinetics model (KM) using calibrated mass transfer coefficients λ_{gw}.*
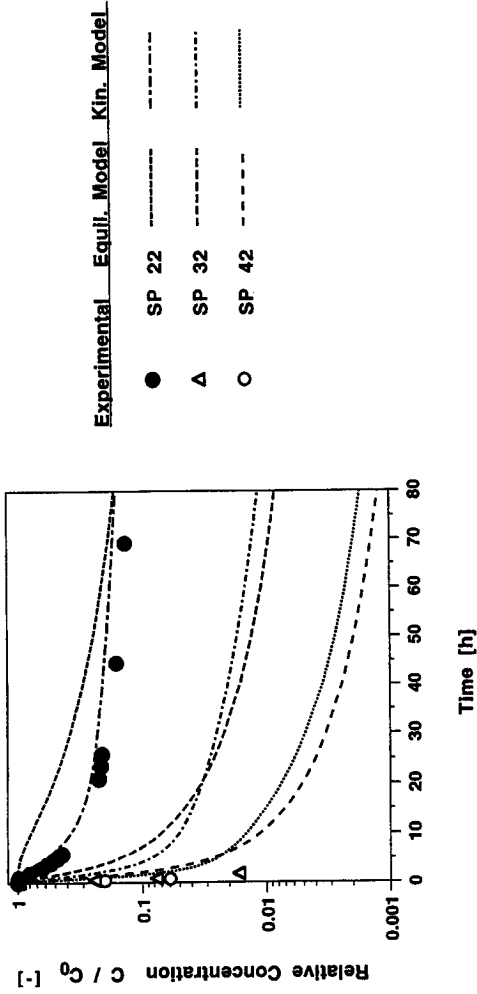
Figure A.11 *Comparison of equilibrium model, kinetics model, kinetics model ($\lambda_{gw} = 10^{-5} s^{-1}$), and experimental gas concentrations obtained for 1,1,1-trichloroethane at different sampling ports (SP) during the wet experiment (V3).*
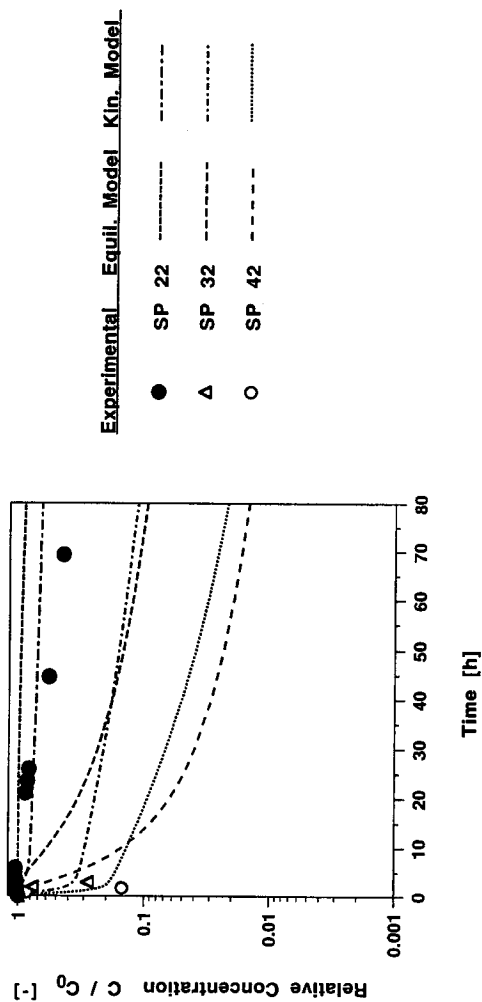
Figure A.12 *Comparison of equilibrium model, kinetics model ($\lambda_{gw} = 10^{-4} \, s^{-1}$), and experimental gas concentrations obtained for 1,1,2-trichloroethane at different sampling ports (SP) during the wet experiment (V3). A value of 0.04 was used as Henry's law constant.*
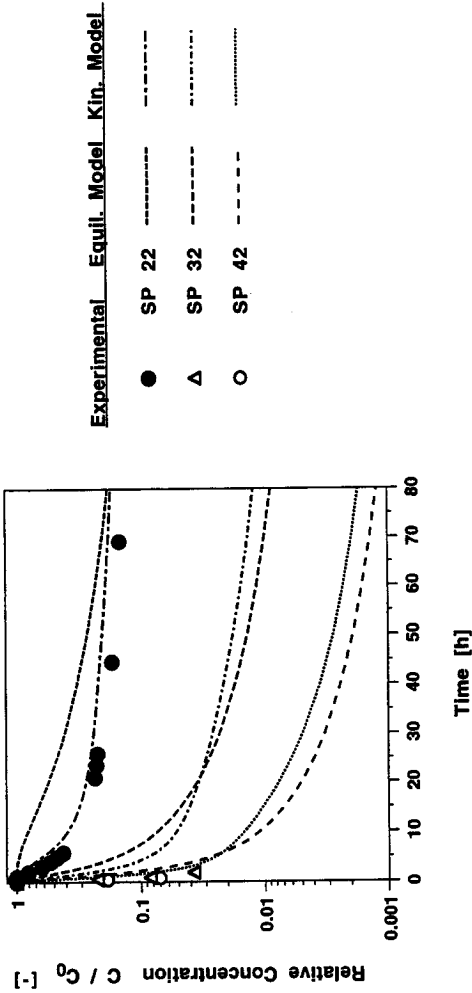
Figure A.13 *Comparison of equilibrium model, kinetics model ($\lambda_{gw} = 10^{-5}$ s^{-1}), and experimental gas concentrations obtained for perchloroethylene at different sampling ports (SP) during the wet experiment (V3).*

NOTATIONS

LATIN SYMBOLS

A	empirical parameter describing the temperature dependence of the Henry's law constant [-]
B	empirical parameter describing the temperature dependence of the Henry's law constant [K]
C_E	concentration at the end of experiment [M L^{-3}]
C_g	concentration in the gas phase [M L^{-3}]
C_g'	relative concentration in the gas phase [-]
C_{gi}	gas concentrations in the different batch types [M L^{-3}]
C_s	sorbed concentration [M M^{-1}]
C_w	concentration in the aqueous phase [M L^{-3}]
C_{wi}	water concentrations in the different batch types [M L^{-3}]
C_0	concentration at time zero [M L^{-3}]
D_0	diffusion coefficient in free air [L^2 T^{-1}]
D_{ij}	dispersion tensor [L^2 T^{-1}]
g	gravitational acceleration [L T^2]
h^*	equivalent fresh air head [L]
h	matric potential head [L]
H_c	Henry's law constant [-]
J_i	mass flux density in i-direction [M L^{-2} T^{-1}]
K_d	solid-water distribution coefficient [L^3 M^{-1}]
k_i	intrinsic permeability [L^2]
k_{rg}	relative gas permeability [-]
k_{rw}	relative water permeability [-]

L	reference length [L]
L_x	reference length in x-direction [L]
$L(C_g)$	differential operator denoting the convective and dispersive terms in the convection-dispersion equation [M L^{-3} T^{-1}]
$L'(C_g')$	dimensionless differential operator denoting the convective and dispersive terms in the convection-dispersion equation [-]
m	empirical parameter in the van Genuchten model [-]
M	total mass in the domain [M]
M_0	total mass in the domain at time zero [M]
M_i	total masses in the different batch types [M]
M_s	mass of sorbent in batch experiments [M]
n	empirical parameter in the van Genuchten model [-]
n_i	unit vector in normal direction to the boundary [-]
N_g	mass-transfer rate per porous medium volume to (+) or from (-) the gas phase [M L^{-3} T^{-1}]
N_s	mass-transfer rate per porous medium volume to (+) or from (-) the solid phase [M L^{-3} T^{-1}]
N_w	mass-transfer rate per porous medium volume to (+) or from (-) the water phase [M L^{-3} T^{-1}]
p	gas pressure [M L^{-1} T^{-2}]
P_D	prefix denominator derived by the SKIT procedure [-]
Pe_{ij}	Peclet numbers [-]
q	Darcy velocity [L T^{-1}]
$|q|$	absolute value of the Darcy velocity [L T^{-1}]
q_i	Darcy velocity in i-direction [L T^{-1}]
R	retardation factor for gas-phase transport [-]
R_s	water-solid retardation factor [-]
S_g	gas saturation [-]
$\overline{S}_g$	effective gas saturation [-]
$S_{g,r}$	residual gas saturation [-]
$S_{g,r}^*$	apparent residual gas saturation [-]

S_w	water saturation [-]
S_o	saturation of liquid organic phase [-]
S_s	specific storativity [T^{-1}]
$\overline{S}_w$	effective water saturation [-]
$S_{w,e}$	gas permeability emergence or extinction point [-]
$S_{w,r}$	residual water saturation [-]
t	time [T]
T	dimensionless time [-]
T_E	dimensionless time at end of experiment [-]
v	average linear velocity [L T^{-1}]
V_{gi}	gas volumes in the different batch types [L^3]
V_{wi}	water volumes in the different batch types [L^3]
v_i	linear velocities in i-direction [L T^{-1}]
V_i	relative velocities in i-direction [-]
x_i	spatial coordinates [L]
X_i	relative distance in i-direction [-]
z	elevation [L]

GREEK SYMBOLS

α	empirical parameter in the van Genuchten model [L^{-1}]
Δp	difference between the gas pressures at the injection and the extraction well [M L^{-1} T^{-2}]
Δx	distance between the two wells of the sand tank [L]
δ_{ij}	Kronecker delta [-]
ε	soil porosity [-]
γ	gas compressibility constant [-]
λ_{gw}	gas-water mass transfer coefficient in the first-order kinetics model [T^{-1}]
λ_L	longitudinal dispersivity [L]

λ_T transversal dispersivity   [L]

μ_g dynamic gas viscosity   [M L^{-1} T^{-1}]

θ_g volumetric gas content   [-]

θ_w volumetric water content   [-]

ρ_0 reference gas density   [M L^{-3}]

ρ_b soil bulk density   [M L^{-3}]

ρ_{rg} relative gas density term   [-]

ρ_w density of water   [M L^{-3}]

τ absolute temperature   [K]

ω Damköhler I number   [-]

ABBREVIATIONS

CDE   convection-dispersion equation

EPICS   equilibrium partitioning in closed systems

LEA   local equilibrium assumption

NAPL   nonaqueous phase liquid

PCE   perchloroethylene (tetrachloroethylene)

SKIT   seperation of the kinetically influenced term

SP   sampling port

SVE   soil vapor extraction

1,1,1-TCA   1,1,1-trichloroethane

1,1,2-TCA   1,1,2-trichloroethane

TCE   trichloroethylene

V1, ..., V4   designation of soil vapor extraction experiment

VOC   volatile organic compound

LIST OF TABLES

LIST OF FIGURES

A.11 - A.13

Comparison of equilibrium model, kinetics model ($\lambda_{gw} = 10^{-5}$ s^{-1}), and experimental gas concentrations obtained for one compound at different sampling ports (SP) during the wet experiment (V3).

REFERENCES

Adenekan, A.E., T.W. Patzek, and K. Pruess, Modeling of multiphase transport of multicomponent organic contaminants and heat in the subsurface: Numerical model formulation, *Water Resour. Res.*, *29*(11), 3727-3740, 1993.

Armstrong, J.E., E.O. Frind, and R.D. McClellan, Nonequilibrium mass transfer between the vapor, aqueous, and solid phases in unsaturated soils during vapor extraction, *Water Resour. Res.*, *30*(2), 355-368, 1994.

Baehr, A.L., G.E. Hoag, and M.C. Marley, Removing volatile contaminants from the unsaturated zone by inducing advective air-phase transport, *J. Contam. Hydrol.*, *4*(1), 1-26, 1989.

Bahr, J.M., and J. Rubin, Direct comparison of kinetic and local equilibrium formulations for solute transport affected by surface reactions, *Water Resour. Res.*, *23*(3), 438-452, 1987.

Ballschmiter, K., W. Haltrich, W. Kühn, and W. Niemitz, HOV-Studie - Halogenorganische Verbindungen in Wässern, Integra-Services, Berlin, 1987.

Bear, J., *Dynamics of fluids in porous media*, Elsevier, New York, 1972.

Bird, R.B., W.E. Stewart, and E.N. Lightfoot, *Transport Phenomena*, Wiley, New York, 1960.

Chiou, C.T., and T.D. Shoup, Soil sorption of organic vapors and effects of humidity on sorptive mechanism and capacity, *Environ. Sci. Technol.*, *19*(12), 1196-1200, 1985.

Croisé, J., J.E. Armstrong, and V. Kaleris, Numerical simulation of rate-limited vapour extraction of volatile organic compounds in wet sands, in *Transport and reactive processes in aquifers, IAHR/AIRH Proc. Ser.*, vol. 5, edited by Th. Dracos and F. Stauffer, pp. 569-575, Balkema, Rotterdam., The Netherlands, 1994.

Croisé, J., W. Kinzelbach, and J. Schmolke, Computation of air flow induced in the zone of aeration during in situ remediaton of volatile hydrocarbon spills, in *Contaminant transport in groundwater, IAHR/AIRH Proc. Ser.*, vol. 3, edited by H.E. Kobus and W. Kinzelbach, pp. 437-444, Balkema, Rotterdam, The Netherlands, 1989.

Damköhler, G., Einflüsse der Strömung, Diffusion und des Wärmeübergangs auf die Leistung von Reaktionsöfen, *Z. Elektrochem., 42*(12), 846-862, 1936.

Dilling, W.L., Interphase transfer processes. II. Evaporation rates of chloro methanes, ethanes, ethylenes, propanes, and propylenes from dilute aqueous solutions. Comparisons with theoretical predictions, *Environ. Sci. Technol., 11*(4), 405-409, 1977.

Fricke, H., Grundwasserverunreinigung durch Herstellung und Anwendung von chlorierten Lösungsmitteln aus der Sicht der Industrie, *DVGW-Schriftenreihe: Wasser, 29*, 119-133, 1981.

Garbarini, D.R., and L.W. Lion, Evaluation of sorptive partitioning of nonionic pollutants in closed systems by headspace analysis, *Environ. Sci. Technol., 19*(11), 1122-1128, 1985.

Gierke, J.S., N.J. Hutzler, and D.B. McKenzie, Vapor transport in unsaturated soil columns: Implications for vapor extraction, *Water Resour. Res., 28*(2), 323-355, 1992.

Gossett, J.M., Measurement of Henry's law constants for C1 and C2 chlorinated hydrocarbons, *Environ. Sci. Technol., 21*(2), 202-208, 1987.

Grathwohl, P., and M. Reinhard, Desorption of trichloroethylene in aquifer material: Rate limitation at the grain scale, *Environ. Sci. Technol., 27*(12), 2360-2366, 1993.

Hayduk, W., and H. Laudie, Prediction of diffusion coefficients for nonelectrolytes in dilute aqueous solutions, *AIChE J., 20*(3), 611-615, 1974.

Horvath, A.L., Halogenated hydrocarbons, Solubility - miscibility with water, Dekker, New York, 1982.

Jennings, A.A., and D.J. Kirkner, Instantaneous equilibrium approximation analysis, *Hydraulic Eng. 110*(12), 1700-1717, 1984.

Johnson, P.C., C.C. Stanley, M.W. Kemblowski, D.L. Byers, and J.D. Colthart, A practical approach to the design, operation, and monitoring of in situ soil-venting systems, *Ground Water Monit. Rev., 10*(2), 159-178, 1990.

Klecka, G.M., S.J. Gonsior, and D.A. Markham, Biological transformations of 1,1,1-trichloroethane in subsurface soils and ground water, *Environ. Toxicol. Chem., 9*, 1437-1451, 1990.

Krause, L.C., Modeling the transport of volatile organic chemicals in unsaturated media: Experimental results, M.S. thesis, MTU, Houghton, 1987.

Kueper, B.H., W. Abbott, and G. Farquhar, Experimental observations of multiphase flow in heterogenous porous media, *J. Contam. Hydrol. 5*, 83-95, 1989.

Leismann, H.M., B. Herrling, and V. Krenn, A quick algorithm for the dead-end pore concept for modelling large-scale propagation processes in groundwater, in *Computational Methods in Water Resources*, vol. 2, edited by M.A. Celia, L.A. Ferrand, C.A. Brebbia, and W.G. Gray, pp. 275-280, Elsevier, New York, 1988.

Lincoff, A. H., and J.M. Gossett, The determination of Henry's constant for volatile organics by equilibrium partitioning in closed systems, in *Gas Transfer at Water Surfaces* by W. Brutsaert and G.H. Jirka (eds.), pp. 17-25, Reidel, Dordrecht, The Netherlands, 1984.

Lingineni, S., and V.K. Dhir, Modeling of soil venting processes to remediate unsaturated soils, *J. Environ. Eng., 118*(1), 135-151, 1992.

Luckner, L., M.Th. van Genuchten, and D.R. Nielsen, A consistent set of parametric models for the two-phase flow of immiscible fluids in the subsurface, *Water Resour. Res., 25*(10), 2187-2193, 1989.

Mackay, D., and W.Y. Shiu, A critical review of Henry's law constants for chemicals of environmental interest, *J. Phys. Chem. Ref. Data, 10*(4), 1175-1199, 1981.

Massmann, J.W., Applying groundwater flow models in vapor extraction system design, *J.Environ. Eng., 115*(1), 129-149, 1989.

McClellan, R.D., and R.W. Gillham, Vapour extraction of trichloroethylene under controlled field conditions, paper presented at Conference on Subsurface Contamination by Immiscible Fluids, Int. Assoc. of Hydrogeol., Calgary, Alberta, Canada, April 1990.

McWhorter, D.B., Unsteady radial flow of gas in the vadose zone, *J. Contam. Hydrol., 5*(3), 297-314, 1990.

Mendoza, C.A., and E.O. Frind, Advective-dispersive transport of dense organic vapors in the unsaturated zone. 1. Model development, *Water Resour. Res., 26(3)*, 379-387, 1990.

Millington, R.J., Gas diffusion in porous media, *Science, 130*, 100-102, 1959.

Mualem, Y., A new model for predicting the hydraulic conductivity of unsaturated porous media, *Water Resour. Res., 12*(3), 513-522, 1976.

Munz, C., and P.V. Roberts, Air-water phase equilibria of volatile organic solutes, *Am. Water Works Ass. J., 79*, 62-69, 1987.

Olschewski, A., U. Fischer, M. Hofer, and R. Schulin, Sulfur hexafluoride as a gas tracer in soil venting operations, *Environ. Sci. Technol., 28*, 264-266, 1995.

Ong, S.K., and L.W. Lion, Mechanisms for trichloroethylene vapor sorption onto soil minerals, *J. Environ. Qual., 20*(1), 180-188, 1991.

Parker, J.C., and A.J. Valocchi, Constraints on the validity of equilibrium and first-order kinetic transport models in structured soils, *Water Resour. Res., 22*(3), 399-407, 1986.

Poulsen, M.M., and B.H. Kueper, A field experiment to study the behavior of tetrachloroethylene in unsaturated porous media, *Environ. Sci. Technol. 26*, 889-895, 1992.

Rao, P.S.C., R.E. Jessup, and T.M. Addiscott, Experimental and theoretical aspects of solute diffusion in spherical and nonspherical aggregates, *Soil Sci., 133*(6), 342-349, 1982.

Rao, P.S.C., R.E. Jessup, D.E. Rolston, J.M. Davidson, and D.P. Kilcrease, Experimental and mathematical description of nonadsorbed solute transfer by diffusion in spherical aggregates, *Soil Sci. Soc. Am. J., 44*(4), 684-688, 1980.

Rippen, G., Handbuch Umweltchemikalien, 3. Aufl., ecomed, Landsberg, FRG, 1990.

Schwille, F., Dense chlorinated solvents in porous and fractured media, Lewis Publishers, Chelsea, Michigan, USA, 1988.

Stauffer, F., and Th. Dracos, Experimental and numerical study of water and solute infiltration in layered porous media, *J. Hydrol., 84*, 9-34, 1986.

Stonestrom, D.A., and J. Rubin, Water content dependence of trapped-air in two soils, *Water Resour. Res., 25*(9), 1947-1958, 1989a.

Stonestrom, D.A., and J. Rubin, Air permeability and trapped-air content in two soils, *Water Resour. Res., 25*(9), 1959-1969, 1989b.

Thorstenson, D.C., and D.W. Pollock, Gas transport in unsaturated zones: multicomponent systems and the adequacy of Fick's laws, *Water Resour. Res., 25(3)*, 477-507, 1989.

Travis, C.C., and J.M. Macinnis, Vapour extraction of organics from subsurface soils - Is it effective ?, *Environ. Sci. Technol., 26*(10), 1885-1887, 1992.

Valocchi, A.J., Validity of the local equilibrium assumption for modeling sorbing solute transport through homogeneous soils, *Water Resour. Res., 21*(6), 808-820, 1985.

van Genuchten, M.Th., A closed-form equation for predicting the hydraulic conductivity of unsaturated soils, *Soil Sci. Soc. Am J., 44*, 892-898, 1980.

Vogel, T.M., and P.L. McCarty, Rate of abiotic formation of 1,1-dichloroethylene from 1,1,1-trichloroethane in groundwater, *J. Conatm. Hydrol., 1*, 299-308, 1987.

Weast, R.C. (ed.), *Handbook of Chemistry and Physics* (70 th. ed.), CRC-Press, Boca-Raton, 1989.

Wehrle, K., and J. Brauns, Column experiments concerning rate limited vapour extraction of volatile organic compounds from wet sands, in *Transport and reactive processes in aquifers, IAHR/AIRH Proc. Ser.*, vol. 5, edited by Th. Dracos and F. Stauffer, pp. 549-554, Balkema, Rotterdam., The Netherlands, 1994.

Wehrle, K, and J. Brauns, Bodenluftabsaugungsverfahren bei CKW-Schadensfällen - Einfluss massgebender Bodenparameter auf die Luftströmung und den Schadstoffaustrag, *KfK-PWAB, 13,* 339-358, 1992.

Wilke, C.R., and C.Y. Lee, Estimation of diffusion coefficients for gases and vapors, *Ind. Chem. Eng., 47*(6), 1253-1257, 1955.

Wilson, D.J., and A.N. Clarke, Soil vapor stripping, in *Hazardous Waste Site Soil Remediation* by D.J. Wilson and A.N. Clarke (Eds.), pp.171-242, Dekker, New York, 1994.

Wolf, K., A. Yazdani, and P. Yates, Chlorinated solvents: Will the alternative be safer ?, *J. Air Waste Manage. Assoc. 41,* 1055-1061, 1991.

Yates, S.R., M.Th. van Genuchten, A.W. Warrick, and F.J. Leij, Analysis of measured, predicted, and estimated hydraulic conductivity using the RETC computer program, *Soil Sci. Soc. Am. J., 56,* 347-354, 1992.

Zurmühl, T., Validierung konvektiv-dispersiver Modelle zur Berechnung des instationären Stofftransports in ungestörten Bodensäulen, Ph.D. dissertation, Bayreuth, FRG, 1994.

ACKNOWLEDGEMENTS

CURRICULUM VITAE

1962	Born on December 4, in Cologne (FRG).
1969 - 1973	Primary school in Cologne-Rheinkassel (FRG).
1973 - 1974	Gymnasium in Cologne-Chorweiler (FRG).
1974 - 1982	Gymnasium in Pulheim-Brauweiler (FRG).
1983 - 1984	Civil service.
1984 - 1989	University of Bayreuth (FRG). Graduation in Geoecology (Diploma).
1989 - 1990	ETH Zurich (Switzerland). Post-graduated program in Urban Water Management and Water Pollution Control.
1990 - 1995	ETH Zurich (Switzerland). PhD study and work as assistant at the Institute of Terrestrial Ecology (Prof. Dr. R. Schulin).